AN ANALYTICAL ANALYSIS OF THE EFFECTS OF INSTANTANEOUS VORTICITY ON COMPRESSOR PERFORMANCE

James Edward Shoemaker

NAVAL POSTGRADUATE SCHOOL
Monterey, California

THESIS

AN ANALYTICAL ANALYSIS OF THE EFFECTS OF INSTANTANEOUS VORTICITY ON COMPRESSOR PERFORMANCE

by

James Edward Shoemaker

Thesis Advisor: Allen E. Fuhs

June 1973

Approved for public release; distribution unlimited.

An Analytical Analysis of The Effects of Instantaneous Vorticity on Compressor Performance

by

James Edward Shoemaker
Ensign, United States Navy
B.S., United States Naval Academy, 1972

Submitted in partial fulfillment of the requirements for the degree of

MASTER OF SCIENCE IN AERONAUTICAL ENGINEERING

from the

NAVAL POSTGRADUATE SCHOOL
June 1973

ABSTRACT

Vorticity forms the basis for a new approach to the analysis of inlet distortion in axial flow fans and compressors. Farmer first formulated this approach and this paper represents a test of the usefulness of his theory. A summary of recent developments in the field along with a discussion of the effects of distortion on stall margin forms a background for this complex problem. A computer program calculates the vorticity pattern at the compressor face using data that are read from a magnetic tape. The data, which were provided by NASA Lewis Research Center in Cleveland, consist of eleven stall events. The output of the program contains tables of stagnation pressure and the partial derivatives of pressure in the R and theta directions as well as three maps. The three maps are of pressure and radial and circumferential vorticity. The results of the program show a correlation between a ring of large positive circumferential vorticity and stall, leading to the conclusion that the stall was caused by the increase in blade loading induced by the vorticity. This conclusion suggests a formulation for a universal inlet distortion index and provides a basis for the evaluation of the vorticity approach to the problem.

TABLE OF CONTENTS

LIST OF TABLES

LIST OF FIGURES

ACKNOWLEDGEMENTS

The author wishes to express sincere appreciation for the patience and guidance of Professor Allen E. Fuhs of the Department of Aeronautics at the Naval Postgraduate School during the completion of this thesis. The author also is grateful for the assistance of Hans Doleman of the W. R. Church Computer Center at the Naval Postgraduate School.

Several persons and organizations provided data and/or assistance for this project. The author wishes to thank Captain Barry Brownstein of AFAPL/WPAFB for his contributions to the development of the computer program. The author also expresses appreciation for the assistance of James Calogeras, Robert Coltrin, Paul Burdstadt and members of the staff at NASA Lewis Research Center in Cleveland, Ohio and for their willingness to supply the data which were used in this thesis.

I. INTRODUCTION

The problem of surge in axial flow fans and compressors in jet engines is a serious one. Unsolved it can result in the loss of a multi-million dollar aircraft and possibly in the loss of the life of the pilot. Manufacturers are therefore forced to design compressors which operate with decreased performance.

During the early years of the use of axial compressors in aircraft jet engines, before high speed flight was a common occurrence, the problem of surge was treated as a steady-state problem with satisfactory results. However, with the advent of high performance and high speed military aircraft, and in particular the F-111 which employed the TF-30 turbo-fan engine, [Ref. 1] it became evident that the problem could no longer be considered to be steady-state. There were some attempts made to improve the steady-state distortion factor, but these were unsuccessful. During the next few years, various attempts were made to develop some sort of a distortion index using the fluctuations of the stagnation pressure as a starting point. These attempts met with some degree of success, but none was the complete answer to the problem.

It has been proposed that a distortion factor which uses vorticity as a measure of instantaneous distortion would provide insight into the fluid mechanics of the problem. Farmer [Ref. 2] first suggested this approach and developed

approximate equations for the vorticity at the compressor face in terms of measured quantities, i.e., stagnation pressure data.

Since most of the distortion factors developed by other researchers were the outgrowth of instantaneous maps of the pressure distribution over the compressor face, it seems logical to take that same route to the development of a distortion index based on vorticity. Therefore a computer program was developed to calculate the instantaneous vorticity pattern and produce the maps of the pattern on the printer component of the computer. This paper will attempt to interpret the output of this program and prove the validity of this approach. Suggestions then will be made concerning the formation of a distortion factor that will allow the prediction of surge for a wide variety of engines.

II. NATURE OF PROBLEM

A. SOME PERTINENT DEFINITIONS

In order to understand the complexity of the problem, one must first be familiar with some of the nomenclature and basic concepts that are used in the field of compressor stability. Brimelow [Ref. 3] gives an excellent presentation of the present theories on this subject as well as a concise explanation of the nomenclature.

The most likely place for an engine to become unstable is in the fan or compressor. These two components are said to be in surge when several or all of the blades become too heavily loaded and are forced to operate in an aerodynamically stalled condition. If one examines the compressor map of the J-85-GE-13 jet engine in Fig. 1, he can see that the conditions for surge are represented by a line on the compressor map. This line is generally called the stall or surge line. The most efficient operating condition of the compressor is as close to this stall line as possible without stalling. In order to insure that the compressor will not surge, it must be run with a safety margin between the operating point and the stall line. The vertical difference between the operating point and the stall line is defined as the stall or surge margin. In today's high performance aircraft it is necessary to have as small a surge margin as possible in order to decrease the specific fuel consumption and increase the total thrust, while building the engine to be as light as possible.

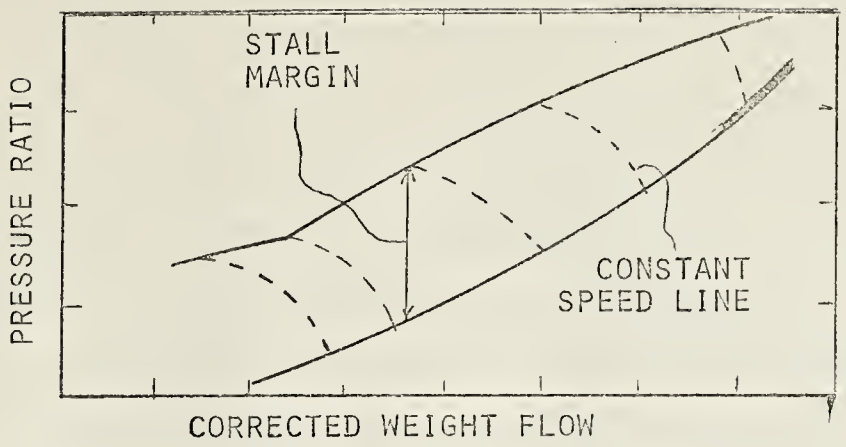

FIG. 1 COMPRESSOR MAP J-85-GE-13

It appears to be an easy task to define a small surge margin and then run the engine at a point such that this surge line will never be crossed. It turns out, however, that the compressor map is only a representation of the steady-state operating conditions of the compressor. Once that fact is known, it is understandable that fluctuations in the flow may affect the stall margin and cause the compressor to stall even though the steady-state operating point may have been well below the stall line.

The term compressor instability may best be defined through visual means. Figure 2 is a hypothetical compressor map with only one constant speed line. On this line six operating points are labeled P1, P2, R1, P3, P4, and R2. If the compressor is operating on the negative slope of this line at point R1, its operation is stable. It is stable because the

operating point will tend to return to R1 if it is forced in either direction along the constant speed line. If it is forced to P2 the mass flow will be decreased. The characteristics of the chamber behind the compressor, which is known as the receiver, require a lower pressure ratio at the reduced mass flow rate. The compressor discharge flow will be forced to expand into the receiver. This will cause an increase in mass flow rate and the operating point will return to R1. In a similar manner if the operating point is forced to P1, it will be forced to return to R1. In this case the pressure ratio will be less than that required by the receiver at the increased mass flow rate and a back pressure will result. The back pressure will cause a reduction in flow rate and the operating point will return to R1.

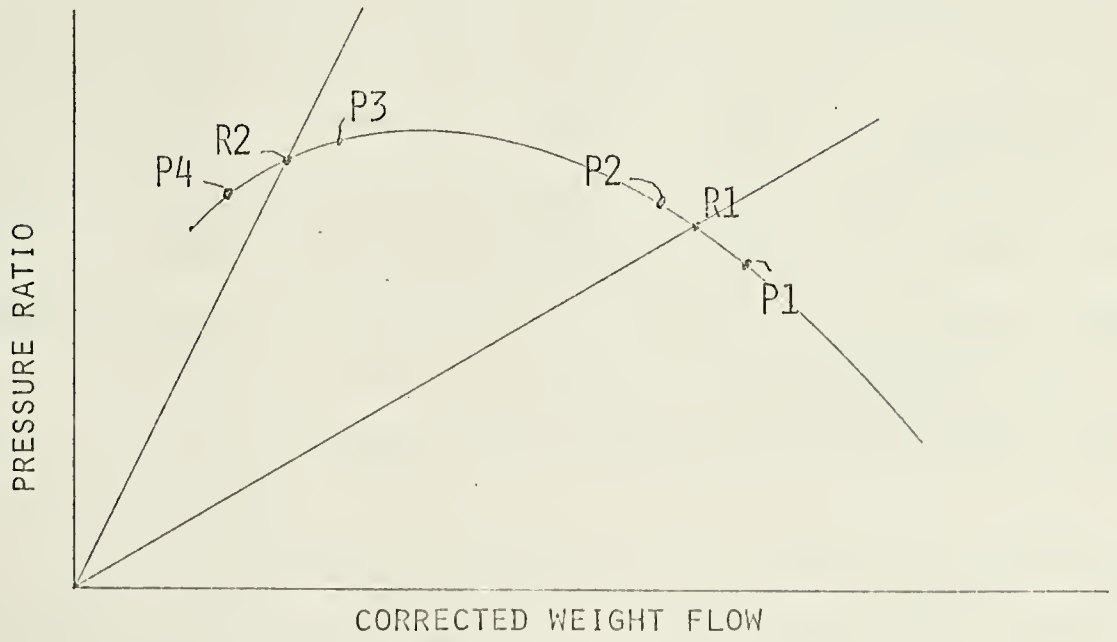

FIG. 2 COMPRESSOR STABILITY

If the compressor is operating on the positive slope of the constant speed line at point R2, the operation of the compressor is unstable. In this case, if the operating point is disturbed from R2, it will continue to move in the direction in which it initially was moving and will not return to R2. If the operating conditions move to point P4, a decrease in pressure ratio will occur. This will in turn set up a back pressure since the pressure in the receiver will be greater than the compressor discharge pressure, and the flow rate will be reduced. The decrease in flow rate will continue to reduce the pressure ratio, and the operating point will continue to move away from R2. If the operating point moves in the other direction along the constant speed line, the pressure ratio will increase which, in turn, will increase the flow rate, and again the operating point will continue to move away from the design point R2.

One can see, therefore, that the limit for stable compressor operation is at the point where the slope of the constant speed line on the compressor map goes to zero. The compressor must operate where the slope of the constant speed line is negative and not be allowed to reach the pressure ratio that corresponds to the limiting point for stable compressor operation.

With high performance aircraft the transient distortions induced by sources external to the engine and in the engine inlet will be of a large magnitude and, therefore, more dangerous to the stability of the compressor. The turbulence

is likely to be generated by some or all of several sources. Some of these sources are: shock waves, boundary layers, hot gases emitted from rockets launched from the aircraft, and off-design operation of the inlet. Since the stall margin is such a critical variable in the operation of a jet engine, it is not feasible merely to increase the stall margin to such an extent that time-variant distortion cannot cause the compressor to stall without a disastrous drop in the overall efficiency of the engine. It is necessary to obtain more information on the source of the distortion, what effect the distortion has on the inlet-compressor interface, and just exactly what type of distortion is most likely to cause a compressor to surge.

B. RECENT DEVELOPMENTS IN THE FIELD

With the advent of the new high performance aircraft it became evident that the method that was used for the evaluation of the inlet-compressor interface was no longer effective. At that time this evaluation had been done wholly by an analysis of the steady-state distortion through the use of a steady-state distortion factor. In a high performance aircraft the inlet flow is more likely to be turbulent making it necessary to evaluate the effects of time variant distortion on the compressor. Since a turbulent flow is a function of four variables, which in a cylindrical coordinate system are R, θ, Z and time, the problem became a much more complex one. The magnitude of the fluctuations in pressure and velocity in a

turbulent flow is such that they cannot be considered small with respect to the steady-state values.

In the light of turbulent inlet flows, it becomes apparent why the steady-state distortion index was not adequate. It does not take the time variable into account. When the inlet flow of a compressor is turbulent, the steady-state distortion factor can be well within the tolerences for stall, and yet the compressor may stall due to the random velocity and pressure fluctuations in the flow.

The first attempt to solve this problem resulted in an improved steady-state distortion factor. As might be expected, however, that factor was also inadequate for the solution of the problem. The amount of turbulence is often quantified by the variation of root-mean-square stagnation pressure ($\Delta P_{rms}/\overline{P}$). Still reluctant to tackle the turbulent flow problem, researchers attempted to devise a method by which the improved steady-state distortion factor could be used with a correlation for the amount of turbulence [Ref. 1]. This method was also ineffective, but it gave some insight into the complexity of the problem.

At this point, it was evident that some method of predicting the effects of time variant distortion must be developed to be used in the inlet-compressor matching problem. The method used was to introduce a system of instrumentation that had a quick response and was able to measure the stagnation pressure at any particular point in time. Measurements then were taken at small intervals of time with probes located on

pressure rakes at the compressor face. The pressures at these discrete points were converted to a distribution and presented in the form of an instantaneous pressure map. By fixing the variable Z at the compressor face, researchers eliminated one variable; and by taking instantaneous pressure readings, they made the problem two-dimensional at any point in time. The influence of time was expressed in the analysis by the time continuity of a set of maps. It became possible to find an empirical correlation between the instantaneous distortion, as represented by the instantaneous pressure map, and surge. In Ref. 5 Calogeras, Burdstadt, and Coltrin found an empirical correlation between the instantaneous pressure distribution and the onset of surge. One of the maps they used in the development of the correlation is depicted in Fig. 3. Using their correlation between the instantaneous pressure distribution and surge, they developed an instantaneous inlet distortion factor with which it was possible to predict stall with some measure of success. This factor was developed for the J-85-GE-13 engine with a particular inlet geometry and was not tested with either other engines or other inlets. It was tested at angle of attack and proved quite successful in that context.

Plourde and Brimlowe [Ref. 6] also developed an instantaneous inlet distortion factor. This factor was used for the TF-30 turbofan engine which is installed in the F-111. It is interesting to note that both of these factors, for the J-85 and the TF-30, are primarily circumferential distortion factors.

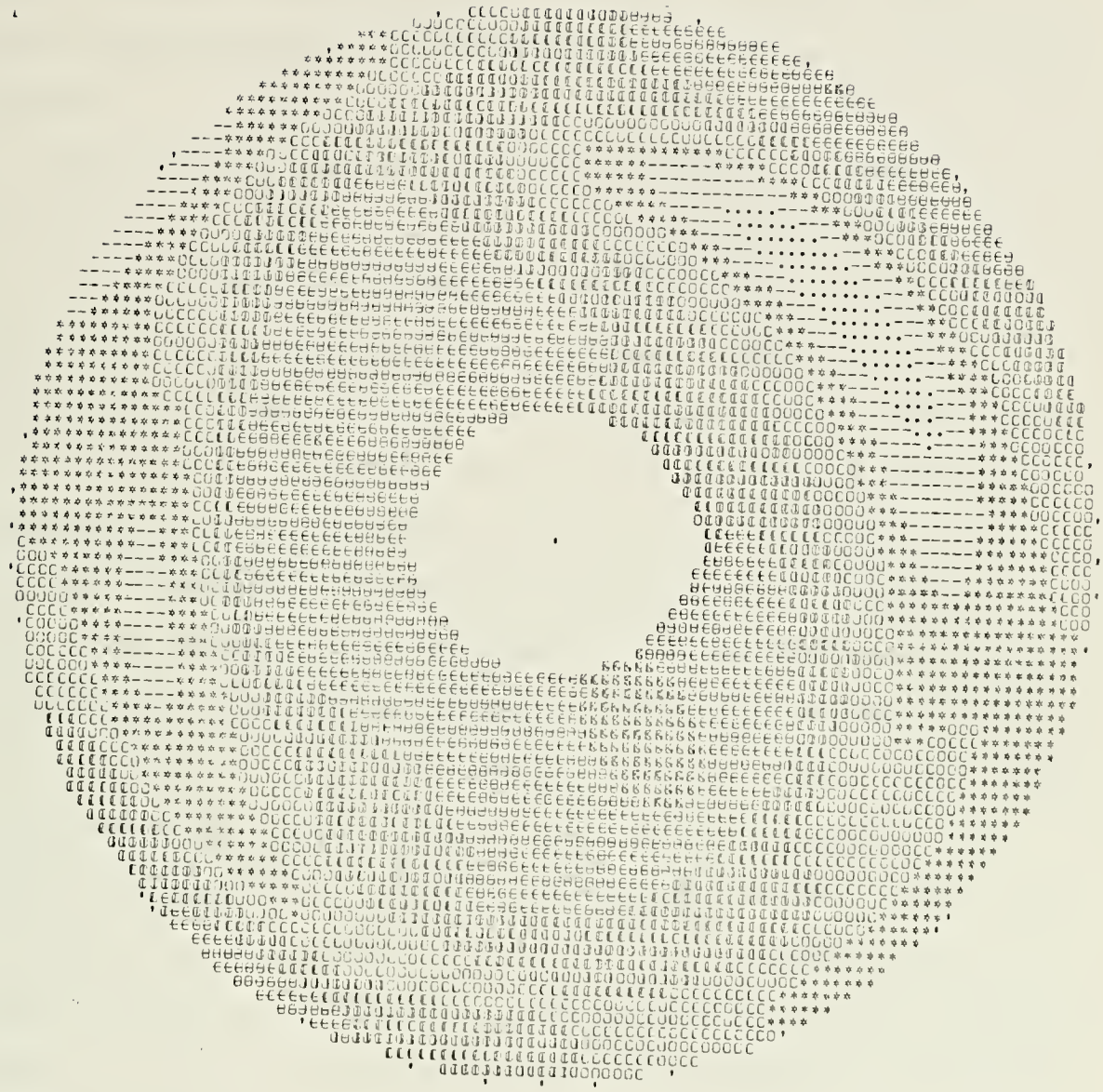

FIG. 3 INSTANTANEOUS PRESSURE MAP

Another interesting point is that while each of these factors is useful in the analysis of the case for which it was developed, neither would be useful, except in a general way, to anyone working on the inlet distortion problem in a different engine.

The period of time for which a particular distortion pattern must persist in order to cause stall was found to be extremely small. Reference 7 states that for the TF-30 this time may be approximately three milliseconds, while Ref. 5 has stated that the time scale for the J-85 can be as short as one millisecond. Reference 8 contains a method of calculating the length of time for which a distortion must persist in order to cause steady-state stall. In general this time, depending on the size of the engine, engine speed, and number of blades, is between one and five milliseconds. If the duration of a distortion is less than this time, stall will not occur, due to dynamic suppression of stall, even though the type of distortion might have caused a stall had it persisted for a longer period of time. Unfortunately the exact time that a distortion must persist cannot be calculated since it may be a function of many more variables than those mentioned above.

Upon examination of several other papers, [9, 10, 11, 12] it becomes evident that the large amount of work that has been done on this problem has resulted in two conclusions. One of these results is an empirical relationship between instantaneous inlet distortion and stall, while the other result is

lack of agreement on the quantitative form of the relationship. As a consequence dozens of instantaneous distortion factors are used at the present time. This lack of consistency can be realized by examining Table I which contains six distortion factors, all of which have been employed for the same engine at various points in time.

TABLE I - DISTORTION FACTORS

$$K=\left[\frac{P_{T2\ AVG}-P_{T2\ MIN\ AVG}}{P_{T2\ AVG}}\right]$$

$$K=\left[\frac{P_{T2\ AVG}-P_{T2\ MIN\ AVG}}{P_{T2\ AVG}}\right]^{.2}\left[\theta-\right]^{.2}\left[\frac{W\sqrt{\theta/\delta}}{W\sqrt{\theta/\delta}_{DESIGN}}\right]10^{2.4}$$

$$K=\left[\frac{P_{T2\ AVG}-P_{T2\ MIN\ AVG}}{P_{T2\ AVG}}\right]\left[\theta-\right]\left[\frac{(\theta+)\ N_{REF}}{(360)\ N}\right]10^{2}$$

$$K=\left[\frac{P_{T2\ AVG}-P_{T2\ MIN\ AVG}}{P_{T2\ AVG}}\right]\left[\theta-\right]\left[\frac{(\theta-)+(\theta+)}{360}\right]10^{-2}$$

$$K=\left[\frac{P_{T2\ AVG}-P_{T2\ MIN}}{P_{T2\ AVG}}\right]\left[\frac{P_{T\ AVG}-P_{T\ MIN}}{2P_{TAVG}-P_{T\ MIN}}\right]\left[2\frac{A_{TL}}{A_T}F(N/\theta)\frac{2A_L}{A_{TL}}\right]$$

$$K=\frac{\sum_{1}^{\infty}\left\{\frac{P_{T2\ AVG}-P_{T2MIN}}{P_{T2\ AVG}}\ \theta-\ C_{RM}\right\}}{C_{RM}}$$

Brownstein [Ref. 13] puts forth a possible universal inlet distortion factor using pressure fluctuations as a base for the index. It appears to have solved some of the problems encountered by earlier factors and is a more general index. This index seems to be very promising. Another, different approach to the problem was put forth by Farmer [Ref. 2] and again in Ref. 8.

C. VORTICITY APPROACH

The approach presented in Ref. 2 and Ref. 8 is new.

Using Crocco's theorem it was possible to obtain an expression for vorticity at the compressor face. Then, with an order of magnitude analysis, using data taken for the J-85-GE-13 jet engine, Farmer was able to eliminate some of the terms involved in the original equation and emerge with a simple, easily calculated expression for vorticity at the compressor face. The two expressions, for radial and circumferential vorticity are

$$\omega'_\theta = \frac{-1}{\gamma P' u'_z} \frac{\partial P'}{\partial r'} \tag{1}$$

$$\omega'_r = \frac{1}{\gamma P' u'_z r'} \frac{\partial P'}{\partial \theta} \tag{2}$$

For a more detailed explanation, consult Farmer's work in Ref. 1. Due to the fact that vorticity lines do not end, i.e., $\nabla \times \omega = 0$, the axial vorticity can be calculated using a control volume. Unfortunately the direction of the axial

vorticity will be ambiguous. As shown in Fig. 4, it is not possible to determine if the axial vorticity enters the control volume from the front or the back.

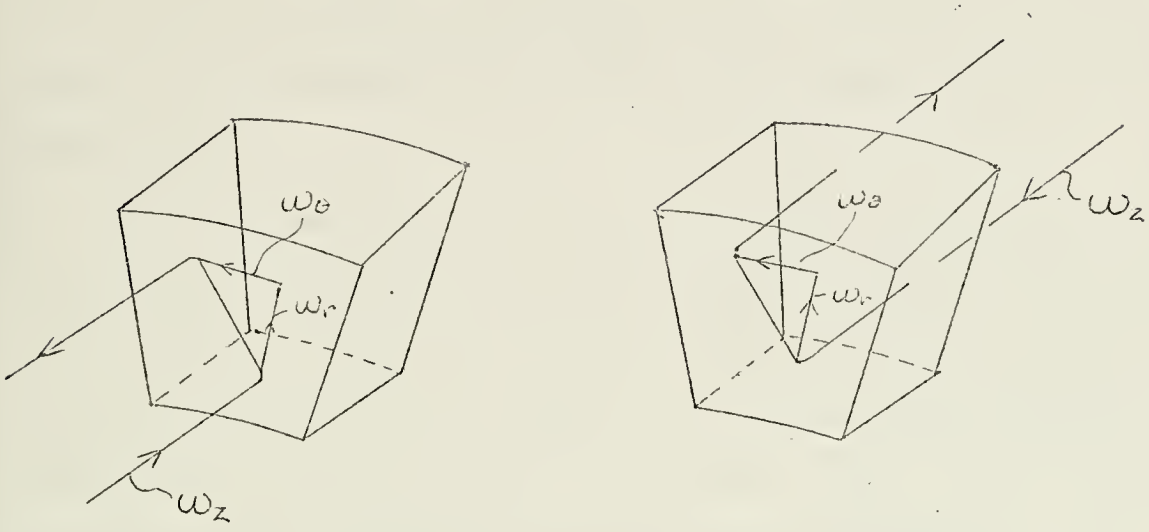

FIG. 4 AMBIGUOUS DIRECTION OF AXIAL VORTICITY

Reference 2 states that circumferential vorticity is likely to have a larger effect on the stall margin than is radial vorticity. This is in concurrence with other work done on this problem, but it may be beneficial to consider the effects of radial vorticity in the light of the fact that the duration of a distortion pattern necessary to cause stall is extremely short. It should be noted, however, that radial vorticity in a rotor is an unsteady phenomenon [Ref. 8] and therefore very difficult to treat.

This new approach seems to have merit, and its usefulness should be tested using some of the large supply of existing data that have been accumulated in the study of this problem.

It would appear that some method of producing instantaneous vorticity maps similar to instantaneous pressure maps would be useful in the evaluation of this theory. Also should the theory be confirmed by these maps, the maps would be instrumental in the formation of a distortion index based on vorticity.

The high speed digital computer is the best choice for the means of production of these maps. The main reason for this choice is the amount of time that would be necessary for their production by hand or even on the most sophisticated desk calculator that is available today. Also, it is necessary that the partial derivatives of pressure in the r' and θ directions be calculated, and this can be done most accurately by the use of numerical curve fitting routines that already have been written for the computer.

The problem then is to develop a computer program that will fulfill the following requirements: read the data from a magnetic tape, define a function in terms of r' and θ that will provide the values of the normalized pressure and its two derivatives at any point on the compressor face, calculate the normalized axial velocity, calculate the radial and circumferential vorticity at any point on the compressor face, and finally print maps of pressure and radial and circumferential vorticity at the compressor face. These requirements are shown more clearly by the flow chart in Fig. 5.

Once the program has been developed and meets the requirements mentioned above, the maps should be interpreted as to

the effect of the instantaneous vorticity distribution on the stall margin. It is hoped that there will be some relationship between the instantaneous vorticity pattern and surge other than the purely empirical correlation between the instantaneous pressure distribution and surge that has been found before.

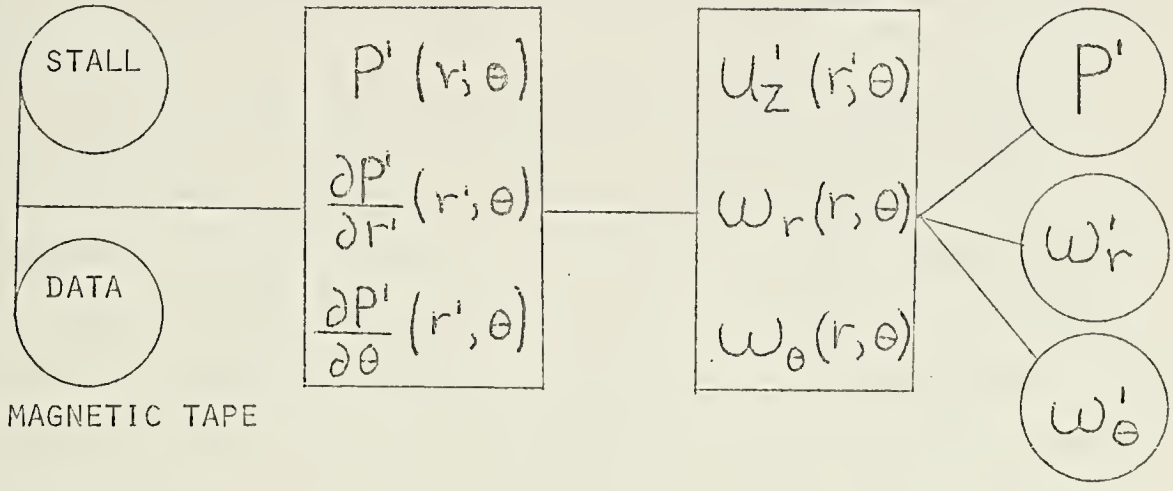

FIG. 5 COMPUTER PROGRAM FLOW DIAGRAM

Farmer, Iverson and Fuhs [Refs. 8 and 14] have presented one such logical relationship between vorticity and stall. It seems that vorticity can cause increased blade loading. Obviously, if the increased blade loading is of a large magnitude and has a sufficiently long duration, this vorticity could be the cause of compressor stall.

If it is not possible to find a logical correlation between instantaneous vorticity and stall, it still might be possible to find an empirical correlation between vorticity

and stall more satisfying than the relationship that has been discovered between instantaneous pressure and stall. This would seem to be a logical expectation since vorticity contains terms of a higher order than pressure and may be a truer measure of distortion.

These two approaches to the interpretation of the vorticity maps both have merit, and both should be considered in this paper.

The discussion of this topic will contain three more considerations. First, it should contain some type of quantitative evaluation of the utility of the instantaneous vorticity distribution in the analysis of inlet distortion. Secondly if the vorticity map proves to be a useful tool, suggestions as to the most beneficial employment of the map in the further study of the problem will be made, and some work will be done on the development of an inlet distortion factor. Finally some insight will be provided into possible alternative paths to the solution of the problem.

III. INTERPRETATION OF VORTICITY MAPS

A. EMPIRICAL APPROACH

A computer program which produces maps of instantaneous vorticity at the compressor face lends itself quite readily to the empirical approach to the interpretation of these maps. It produces a large number of maps that are easily examined. If a pattern of vorticity is present in several of the events just prior to stall, and not present at other times, it is likely that the pattern represents the distortion which was the cause of compressor surge. In the examination of these maps it is necessary to consider the duration of the pattern which seems to be causing surge. If the pattern does not persist for a sufficient length of time, its effects on the compressor are likely to be minimized by dynamic suppression of stall. It is possible to compute a number, known as the reduced frequency, which will provide some insight into the influence of dynamic suppression on a distortion pattern's ability to cause compressor surge. Equation (3), from Ref. 14,

$$\text{Reduced Frequency} = \frac{\pi f C}{U} \qquad \begin{array}{l} C = \text{chord} \\ U = \text{tip speed} \end{array} \qquad (3)$$

is the equation for reduced frequency. For the J-85 the length of time that a pattern must exist in order to be relatively free from the influence of dynamic suppression of stall is approximately one millisecond. This number, however, is more of an order of magnitude approximation than a hard

and fast rule. It could be that a particularly strong distortion pattern with a duration of slightly less than one millisecond would be quite capable of inducing stall in the compressor. For a more complete explanation of dynamic suppression of stall, consult Carta [15], Erikson and Redding [16] and Carta [17].

Examination of the maps generated by the computer program leads to the conclusion that the radial vorticity pattern is unlikely to yield an empirical correlation to stall or least not one that is evident through visual inspection. The pattern of radial vorticity is generally quite random, and the same pattern does not persist for more than a fraction of a millisecond. Figure 6 contains one of the radial vorticity maps drawn by the program. Figure 8 contains the scale to be used in examination of the maps. The numerical values in Fig. 7 are the values of the constant normalized vorticity lines that are represented by the boundary between the two symbols on either side of the number. This scale is the same for all maps of vorticity that are presented in this thesis.

The patterns of instantaneous circumferential vorticity prove much more enlightening. The maps in Figs. 8 - 11 are patterns that appear prior to stall in the first four of the eleven stall events.

The ring of large positive vorticity at the tip of the blades and extending nearly an entire 360 degrees seems to be quite likely to have caused stall. It is not feasible to

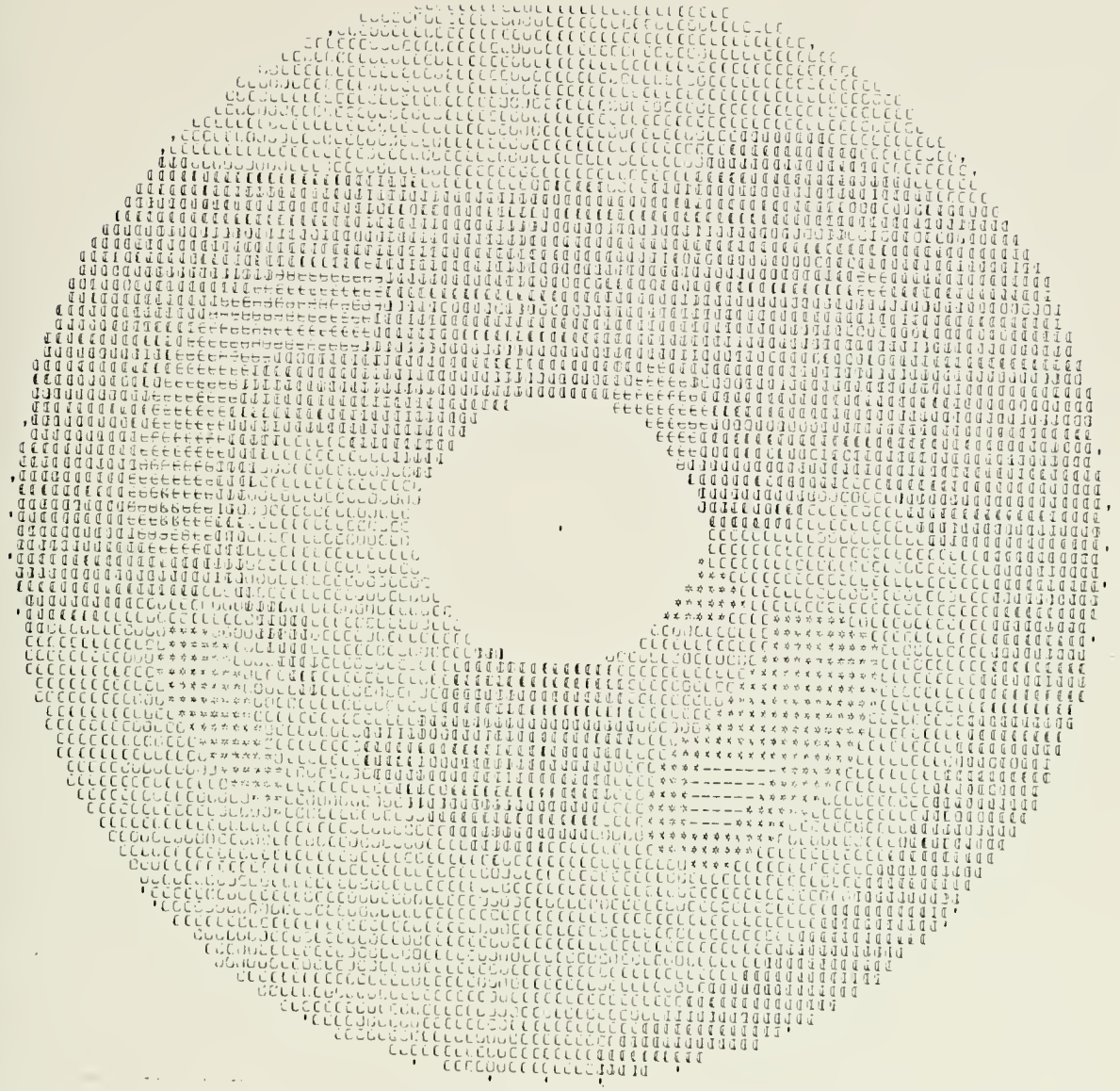

FIG. 6 INSTANTANEOUS RADIAL VORTICITY MAP

FIG. 7 SCALE FOR VORTICITY MAPS

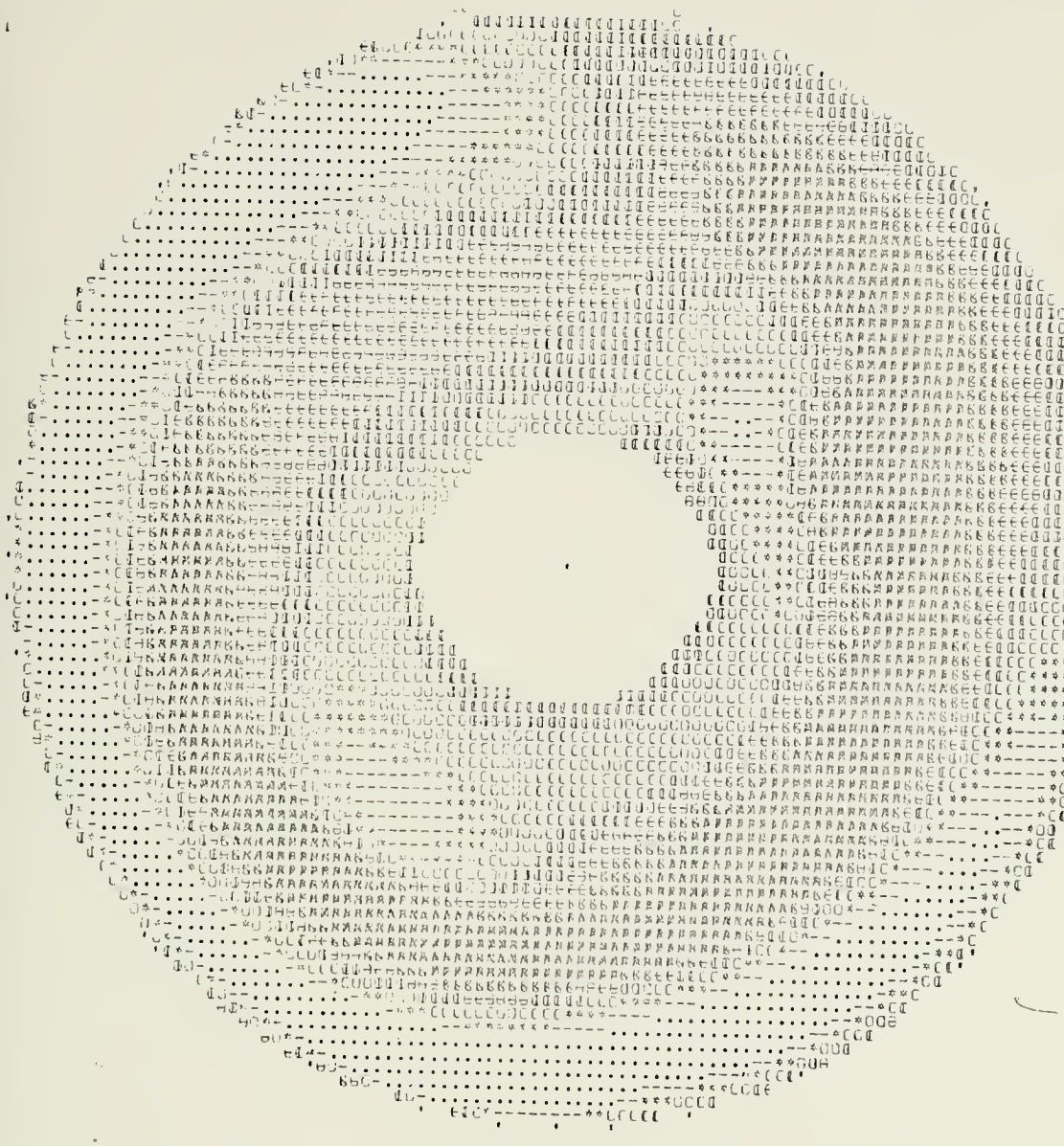

FIG. 8 CASE I CIRCUMFERENTIAL VORTICITY

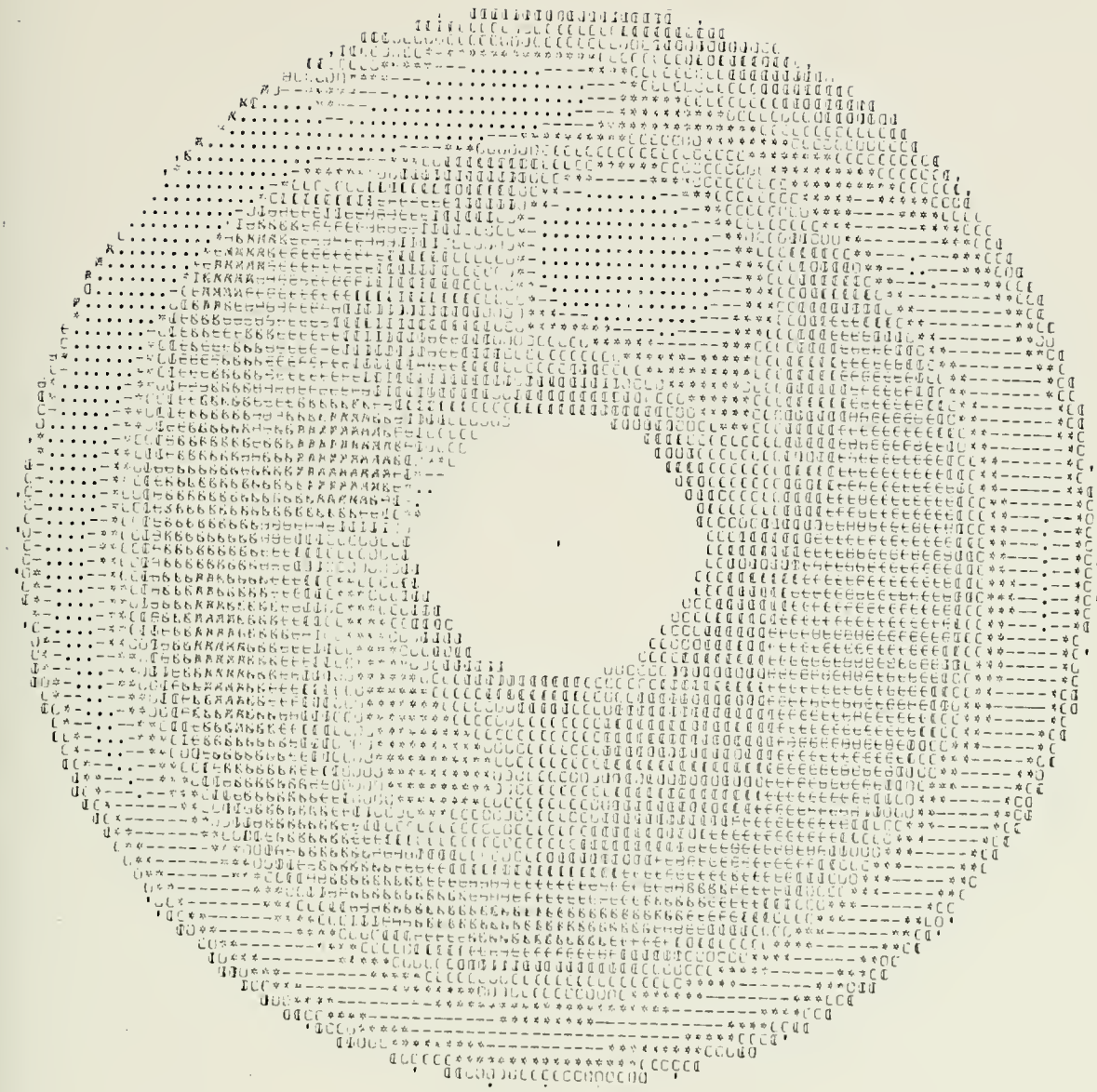

FIG. 9 CASE II CIRCUMFERENTIAL VORTICITY

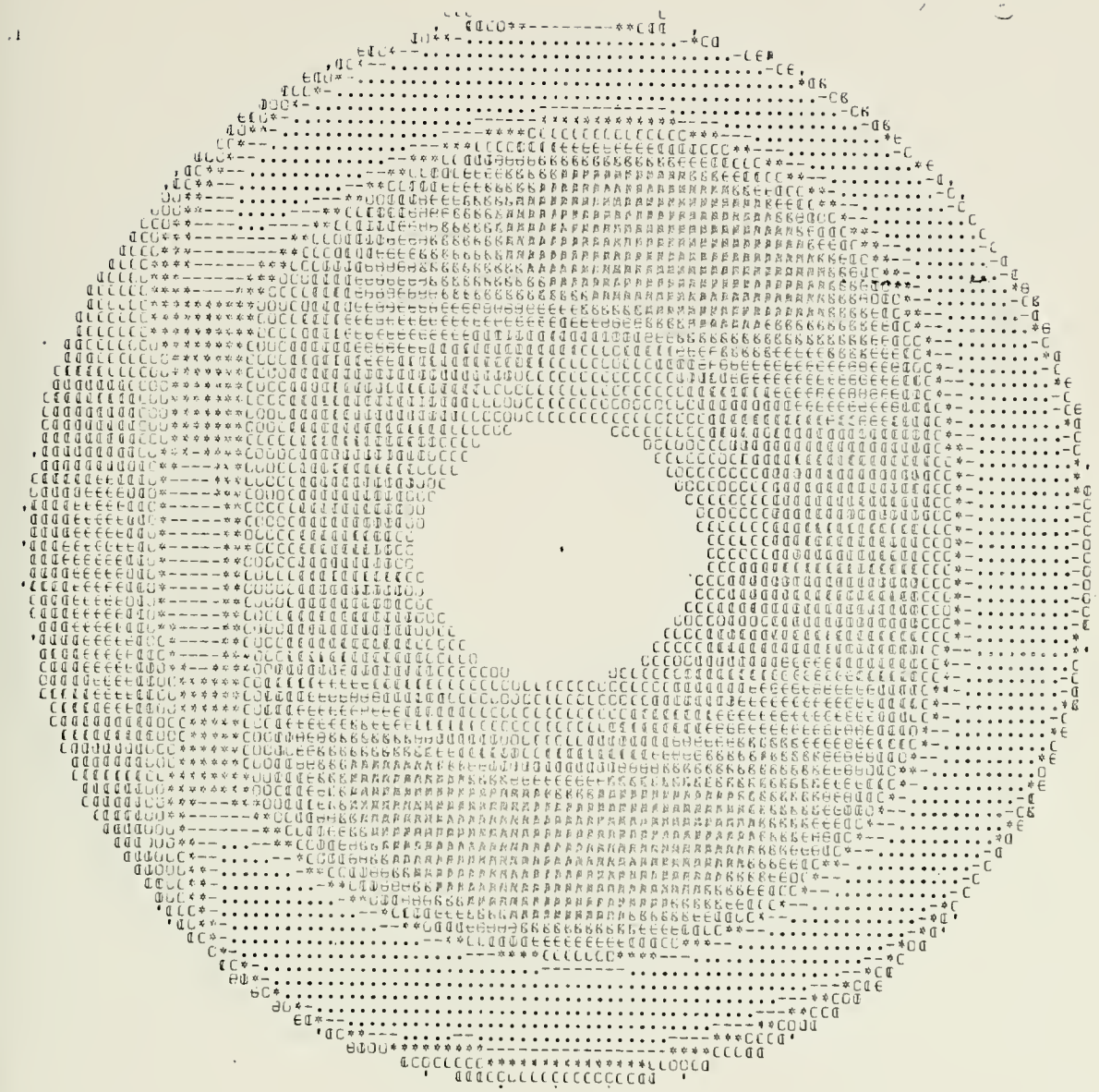

FIG. 10 CASE III CIRCUMFERENTIAL VORTICITY

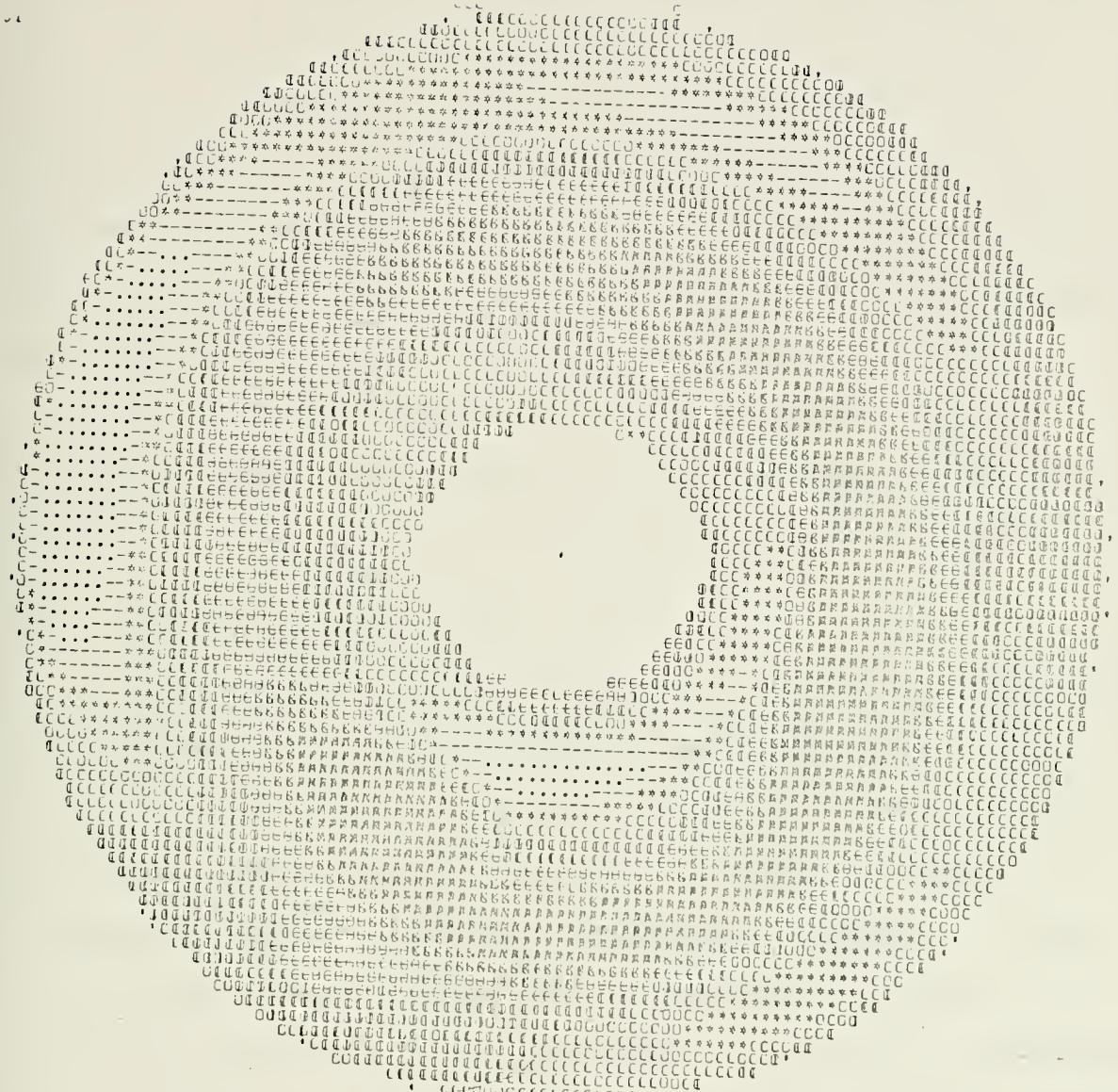

FIG. 11 CASE IV CIRCUMFERENTIAL VORTICITY

examine every map in a stall event, due to the amount of computer time required for the production of these maps; each set of three maps requires 50 seconds of computer time. With 2048 sets of three maps per stall event, this would amount to 28 hours of computer time for each event. A random sampling of vorticity maps was taken, and the ring pattern does not appear except at such a time that it could be the cause of stall. The similarities between these maps are striking. A distortion index based on this pattern could yield some insight into how the compressor stalls. It would appear from this pattern that the tips of the blades are the cirtical point of the compressor for the J-85.

B. ANALYTICAL APPROACH [Ref. 8]

There has been a large amount of work done for predicting the effects of nonuniform flows on the performance of a cascade. Reference 8 contains an excellent summary of some of the results of this work as well as sample calculations of the effects of secondary flow on blade loading. Further insight into these effects can be gained by consulting Ref. 14.

The primary effects of radial vorticity can be understood easily. Refercnce 18 states that an airfoil can be represened by a reentrant vortex. It is fairly easy to see that the blades in a compressor could be approximated by a group of negative radial vortices. (See Fig. 12). It is then a logical supposition that positivc radial vorticity would tend to decrcase the bladc loading and negativc radial vorticity would tend to increase blade loading, as in Fig. 13. The trouble

with this observation is that radial vorticity in a rotor is an unsteady phenomenon. Table II classified types of vorticity in a rotor and stator as steady or unsteady.

FIG. 12 EQUIVALENCE OF BLADE CIRCULATION AND VORTICITY

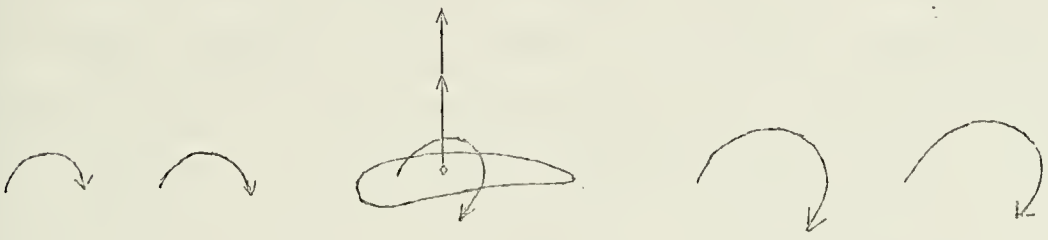

FIG. 13 ADDITIONAL LIFT DUE TO RADIAL VORTICITY

TABLE II. POSSIBLE COMBINATIONS IN A ROTOR [Ref. 8]

Vortex	Direction of Vortex	Flow
Sheet	Radial	Unsteady
Filament	Radial	Unsteady
Filament	Circumferential	Unsteady
Sheet	Circumferential	Steady

The influence of circumferential vorticity on blade loading is not so clear. In Ref. 8 the secondary effects of one vorticity pattern were calculated with the following results. It was found that circumferential vorticity could cause additional blade loading through its secondary flow effects. The vorticity pattern for which these effects were calculated is remarkably similar to the pattern that the empirical correlation has tentatively singled out as the cause of compressor surge. This pattern is depicted in Fig. 14. In Fig. 15 the induced downwash from this vorticity pattern is pictorialized. If the blade tips were highly loaded, the additional lift caused by the circumferential vorticity definitely would be large enough to initiate stall. It seems, therefore, that there is a logical relationship between a ring of large positive vorticity at the tip and stall that concurs with the purely empirical correlation which was pointed out in the previous section. For a thorough explanation of the method of calculation of these secondary effects, consult Ref. 8 or Ref. 1.

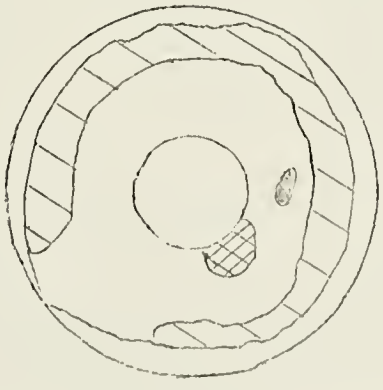

FIG. 14 VORTICITY PATTERN

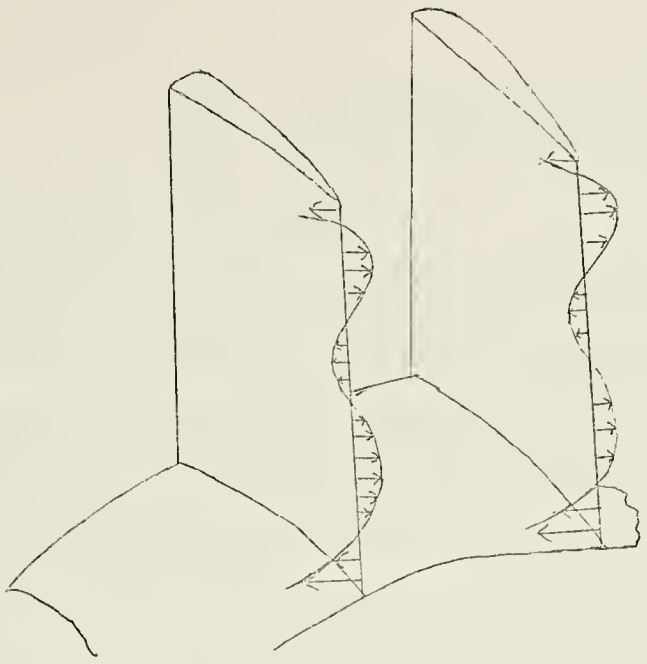

FIG. 15 INDUCED DOWNWASH [REF. 8]

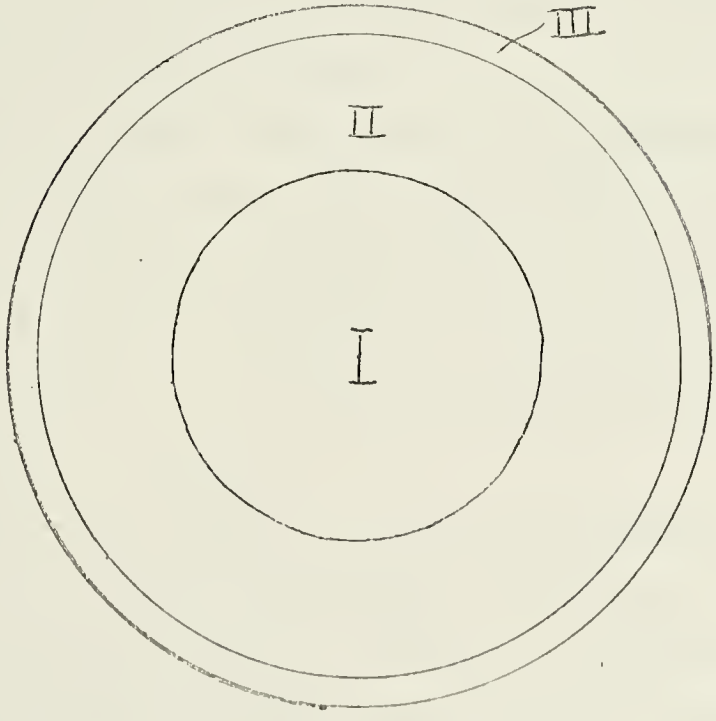

FIG. 16 REGIONS OF COMPRESSOR FACE

IV. A DISTORTION INDEX

A. DEVELOPMENT OF THE INDEX

From the two approaches to the interpretation, it has been seen that stall in the J-85 is probably caused by a type of distortion which is characterized by a large negative vorticity at the midspan and a large negative vorticity at the tip. Both interpretations point to this conclusion, making it fairly certain that this path of investigation will bear fruit. In order to investigate the problem further and to determine if the conclusion that stall is caused by that one particular vorticity pattern is correct, it would be helpful to develop a distortion index based on the assumption that that pattern causes stall.

The distortion index will have certain advantages over the maps. The most important of these is that it will take less computer time and will facilitate the processing of more data. This will make it possible to evaluate data for which no map was produced and to check the conclusion made in the interpretation of the maps.

The index should fulfill certain requirements. It should be large when the vorticity pattern, tentatively labeled as the stall producing pattern, is present and smaller when it is not. It should be large only if the pattern persists for one millisecond or more, since if it does not persist for that long, it is unlikely that it would have produced stall.

Since this is the first index ever devised based on vorticity, there is no guideline as to what is large and what is small. This is an advantage in that it does not matter how large the index is. It is only the relative size at different points in time that is of interest. However, it will be possible to get some feel for the size of this index which causes stall through the comparison of the index for different stall events.

The development of the index will now be described. Through inspection it was seen that the positive ring of vorticity was generally at r' of greater than 0.75, and the negative ring of vorticity was at r' of less than 0.75. The boundary layer had dominated the vorticity at r' greater than 0.95. At r' less than 0.5, there was very little regularity to the pattern. In order to reduce computer time, it was decided to employ the observations above and to make the index a simple arithmetic summation with as little testing for magnitude as possible. To this end, the vorticity map was separated into three sections as shown in Fig. 16. Region I at r' less than 0.5 was ignored. In region II, the vorticity at radii of 0.55, 0.60, 0.65, and 0.70 was found for θ of 0 to 360 at steps of 0.5°, and summed yielding equation (4).

$$F_{ACTI}(t) = \sum_{N=1}^{719} [V_{ORT}(.55, NX.5) + V_{ORT}(.60, NX.5) + V_{ORT}(.65, NX.5) + V_{ORT}(.70, NX.5)] \quad (4)$$

If the vorticity at any point in this region was greater than 0, it was rejected. In region III, the positive vorticity at radii of 0.8, 0.85, 0.90, and 0.95 was found and summed. In this case negative numbers were rejected. This yields equation (5).

$$F_{ACT2}(t) = \sum_{N=1}^{719} \left[V_{ORT}(.80, N\Delta.5) + V_{ORT}(.85, N\Delta.5) + V_{ORT}(.90, N\Delta.5) + V_{ORT}(.95, N\Delta.5) \right] \quad (5)$$

The distortion factor is then the difference between these two sums, (equation 6).

$$F_{ACT}(t) = F_{ACT2}(t) - F_{ACT1}(t) \quad (6)$$

At this point, a distortion factor was known at each instant of time. If the ring of positive vorticity at the tip is present along with the ring of negative vorticity at the hub, this index should be a large number. However, this number carries no information about the duration of the pattern. In this simple development the time factor was incorporated in the following manner. The distortion factor for each case was multiplied by the distortion factor 0.625 ms. before it and 0.625 ms. after it. In this manner a new distortion factor is calculated that reflects the vorticity pattern as seen through a "window" that is 1.25 milliseconds long. This is a simple matter to program since the cases used are all 0.625 milliseconds apart. The distortion factor becomes

$$K_{DIST} = F_{ACT}(t - .625\ ms) \times F_{ACT}(t) \times F_{ACT}(t + .625) \quad (7)$$

In this manner a particular distortion must last at least 1.0 millisecond in order to yield a large value of the distortion factor.

B. TEST OF THE DISTORTION FACTOR

The distortion factor was inserted into the computer program and tested for several stall events. A graphical representation of the results of each of the first four events is presented in Figs. 17-20.

It can be seen that the distortion factor is quite effective for three of the four cases. In the fourth case, however, it gives no indication whatsoever of stall. This could be due to one or all of several influences. The index fails to account for several things. It could be that the index becomes large at the wrong time due to the fact that there may be a ring of positive vorticity at the tip and negative vorticity at the midspan without the increase in lift if they do not coincide as shown in Fig 21. If this is the case, they could cause the index to be large without inducing stall. Also, there may be other influences, that are at the present obscure, which play a part in the stall of a compressor. Finally, it could be that a mild distortion can cause stall if it persists for long enough.

Another interesting point about the test is that for two of the three successful tests the peak of the distortion index which seems to have initiated stall is of the same order of magnitude, while the third is much smaller. This seeming discrepancy could provide some insight into the mechanism of stall. The operating points for the four cases were plotted on a performance map for the J-85, and the steady-state

operating point for the case in which a smaller peak in distortion index initiated stall is much closer to the surge line than the other two successful tests. This may be a significant observation.

In any case, if the conclusions that lead to the distortion index are correct, then the initial level of distortion is not the same for all operating conditions of the compressor. Also, there is something about that particular operating point for the fourth case that makes the compressor more susceptible to stall.

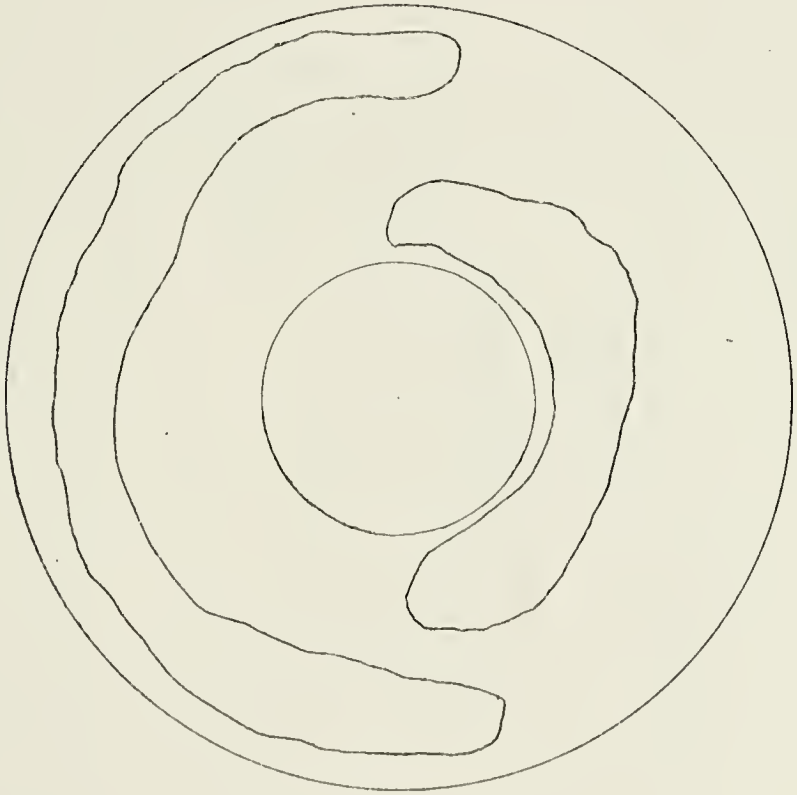

FIG. 21 VORTICITY PATTERN PRDUCES LARGE INDEX, NO STALL

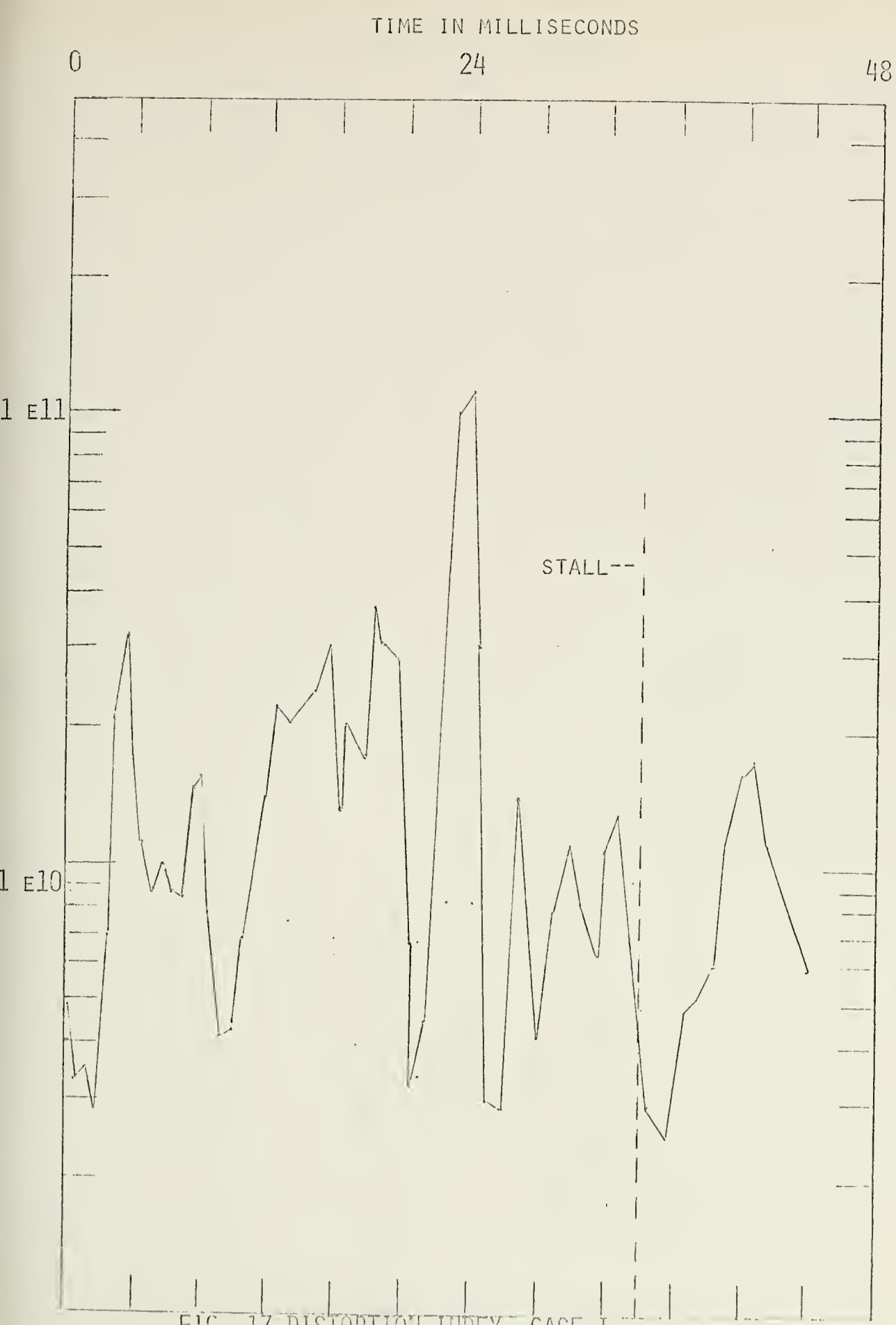

FIG. 17 DISTORTION INDEX, CASE I

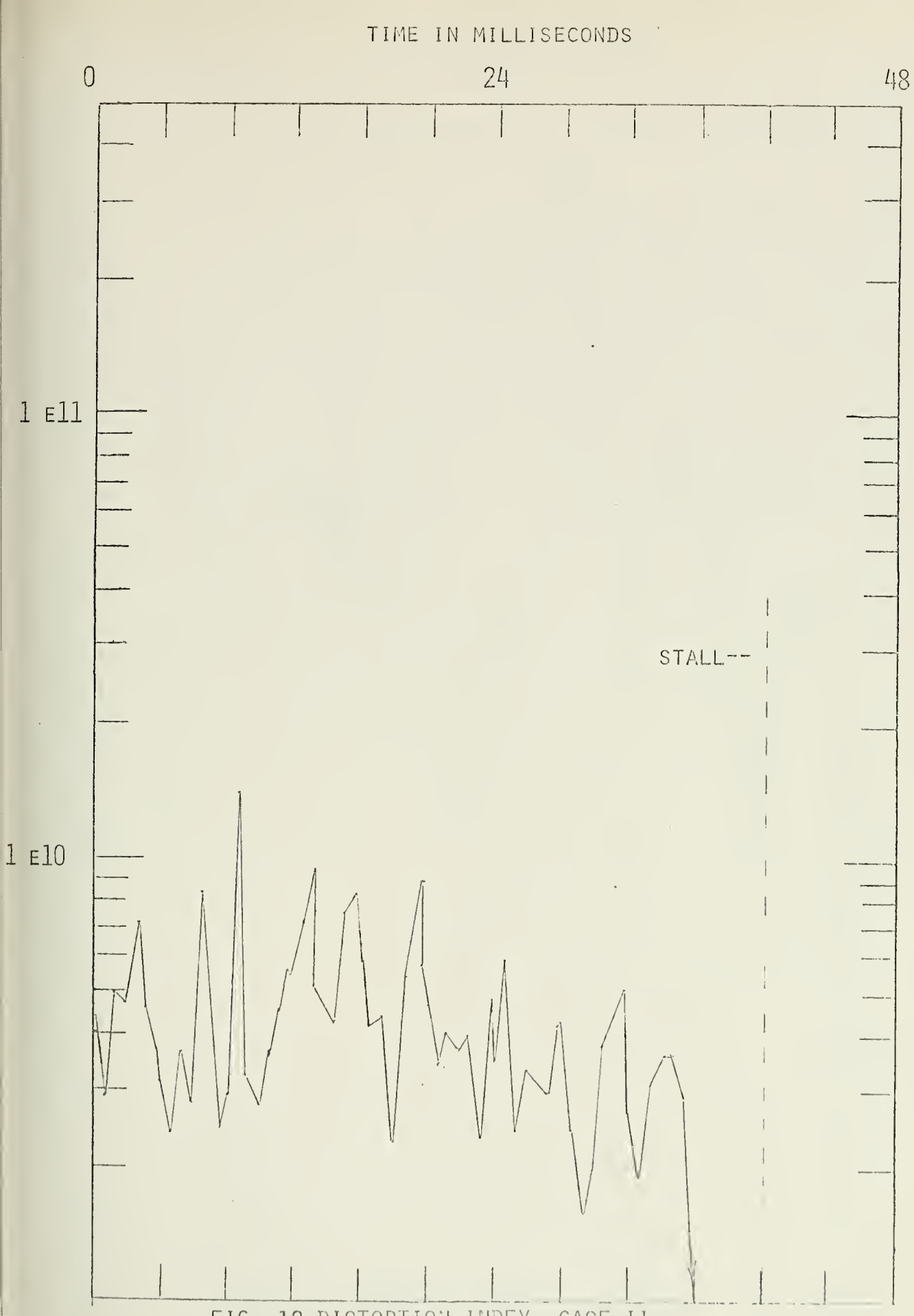

FIG. 18 DISTORTION INDEX, CASE II

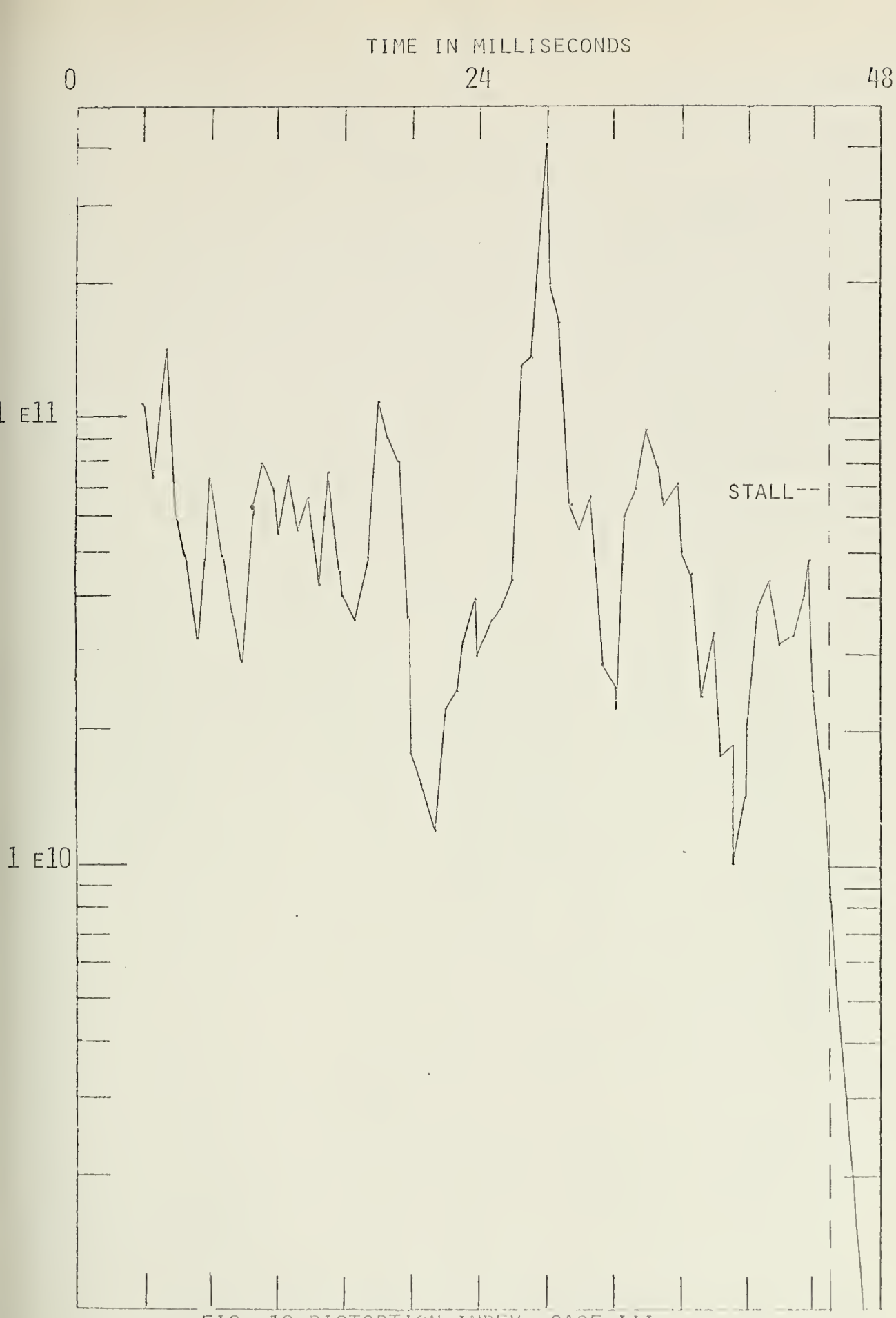

FIG. 19 DISTORTION INDEX, CASE III

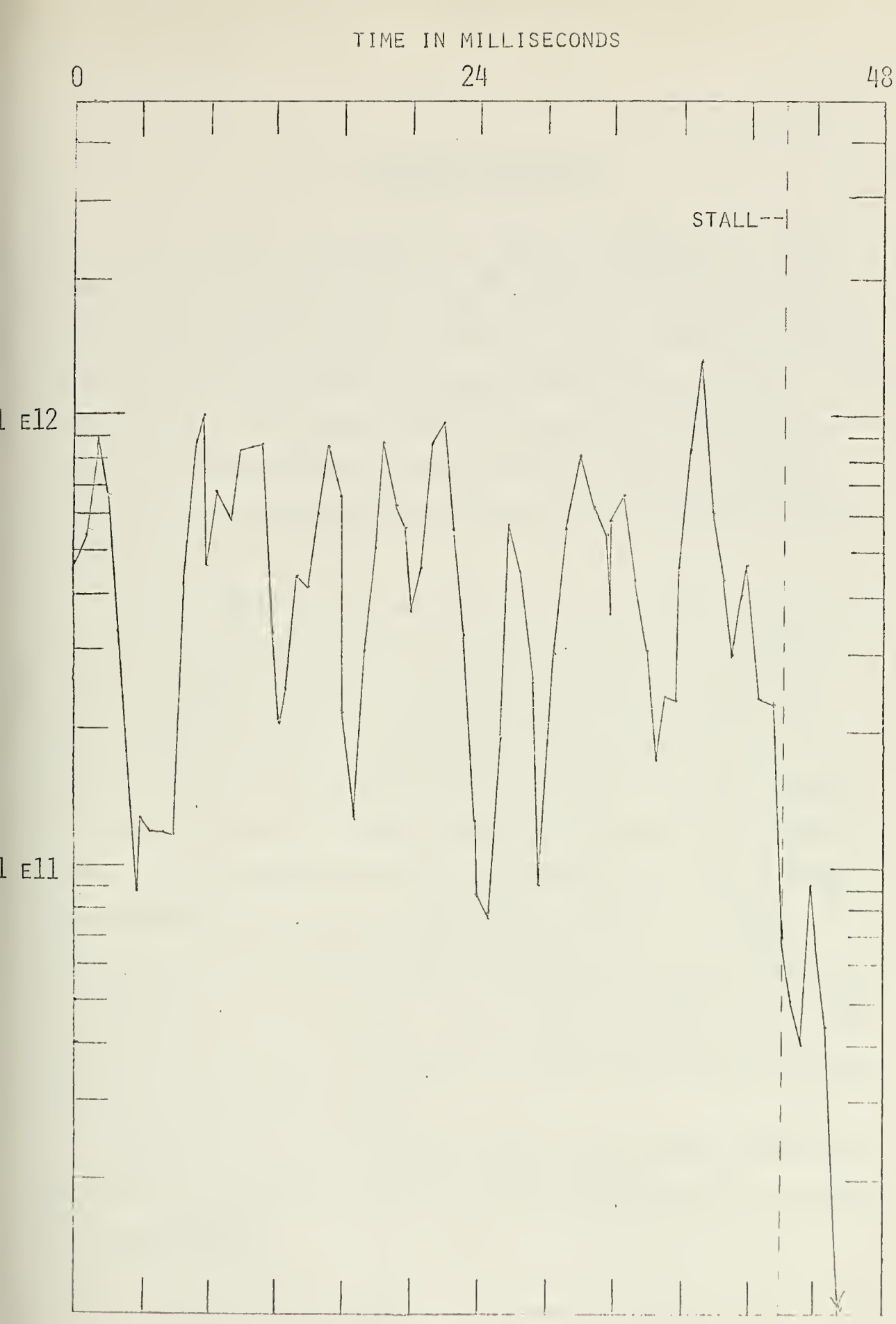

FIG. 20 DISTORTION INDEX, CASE IV

V. SUMMARY AND REVIEW

In review it is necessary to put the findings of this thesis in perspective. In order to test the usefulness of the instantaneous vorticity approach to the problem of inlet distortion in axial flow compressors, the pressure distribution at the compressor face must be converted to a vorticity distribution at the compressor face. A computer program was developed which performed this task with reasonable accuracy.

Once the program was operational it was used to convert instantaneous pressure data for the J-85-GE-13, which was taken in the 10 x 10 foot supersonic wind tunnel at NASA Lewis Research Center in Cleveland, Ohio, into vorticity maps of radial and circumferential vorticity at the compressor face. The map of radial vorticity offered little information, but a marked empirical relationship was found between a circumferential vorticity pattern and stall. A crude instantaneous distortion index was defined using this empirical relationship as a criterion. The results of these tests show that there is indeed an empirical relationship between instantaneous vorticity and stall.

The tests of the distortion factor also showed that this pattern of vorticity is not the only mechanism that is capable of causing stall.

VI. CONCLUSIONS

The primary purpose was to establish the validity of the vorticity approach to the problem of instantaneous distortion in a jet inlet. This approach to the problem has proved to be quite useful in understanding the effects of distortion on the stability of a compressor. The computer program which converts the pressure distribution at the compressor face to the vorticity pattern at the compressor face will be instrumental in further research along this line of reasoning.

While the crude distortion factor developed in this work is fairly successful in the prediction of stall, and could most likely be refined to be even more effective, it is not the purpose of this line of research to determine an empirical instantaneous distortion pattern for the J-85. The data for the J-85 were used to show that the vorticity approach to the problem is valid. The overall purpose of the research is to develop a universal inlet distortion factor that could be employed for a wide variety of engines and airframes. Further research should be along these lines.

It may be possible to make progress toward a universal inlet distortion factor through the calculation of the theoretical secondary flow effects of vorticity as it passes through the compressor. In further work the radial and axial vorticity must be incorporated into the analysis. Other factors that must be considered in the analysis include

blade twist and type of blading. Finally, as stated in Ref. 2, other types of distortion, such as temperature distortion, must be considered. The vorticity approach to the problem of inlet distortion is very promising and may provide the reliable universal distortion criteria that industry lacks today.

APPENDIX A

EXPLANATION OF DATA

The data used by the computer program are the same data which were used in Ref. 5. They were taken in the 10 x 10 foot supersonic wind tunnel at NASA Lewis Research Center in Cleveland. They consist of eleven different stall events. For each stall event the 250 milliseconds of analog data prior to stall were digitized at 8000 points/second/channel. A schematic of the digitizing system is in Fig. A-1. Each of the digitized values consists of only the fluctuating component of pressure, so the steady-state values of pressure just prior to stall must be used in order to find the absolute total pressure at each point. The steady-state value was not used alone, however. Instead a reference pressure which includes a correction for the leakage of the high pass filter was added to the fluctuating component to obtain absolute values of the stagnation pressure. The reference pressure was determined in the following manner. Analog data for all thirty channels were filtered at 50 hertz. A drawing of the compressor face with the positions of all the probes is shown in Fig. A-2. A five second section of data prior to stall was digitized at 200 points/second/channel. The thousand values for each channel were then averaged to find delta p average for each channel, where delta p average is equal to the filter leakage. The values of P_{ref} and dP/dt then were calculated using equations A-1 and A-2.

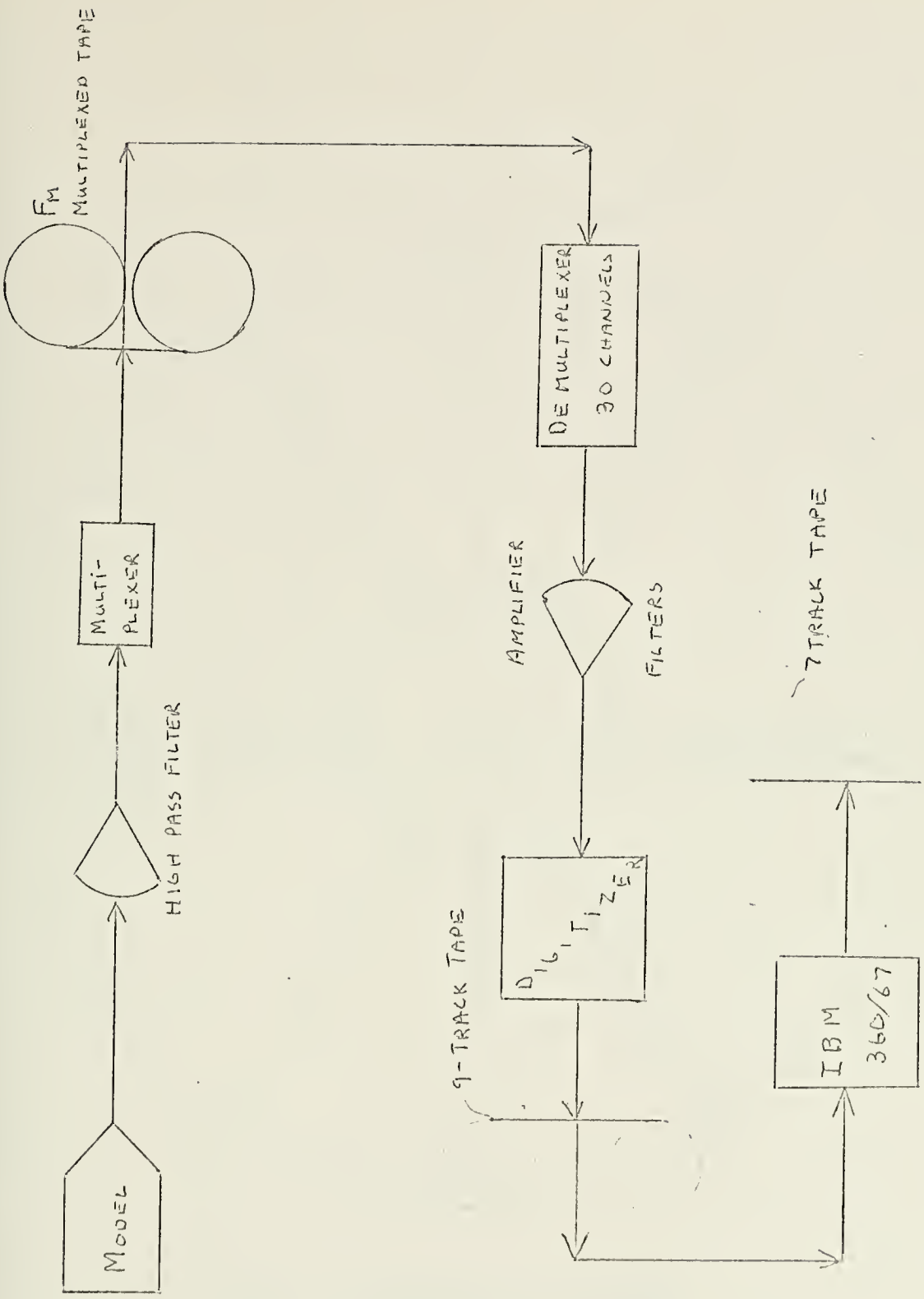

FIG. A-1 SCHEMATIC OF DIGITIZING SYSTEM

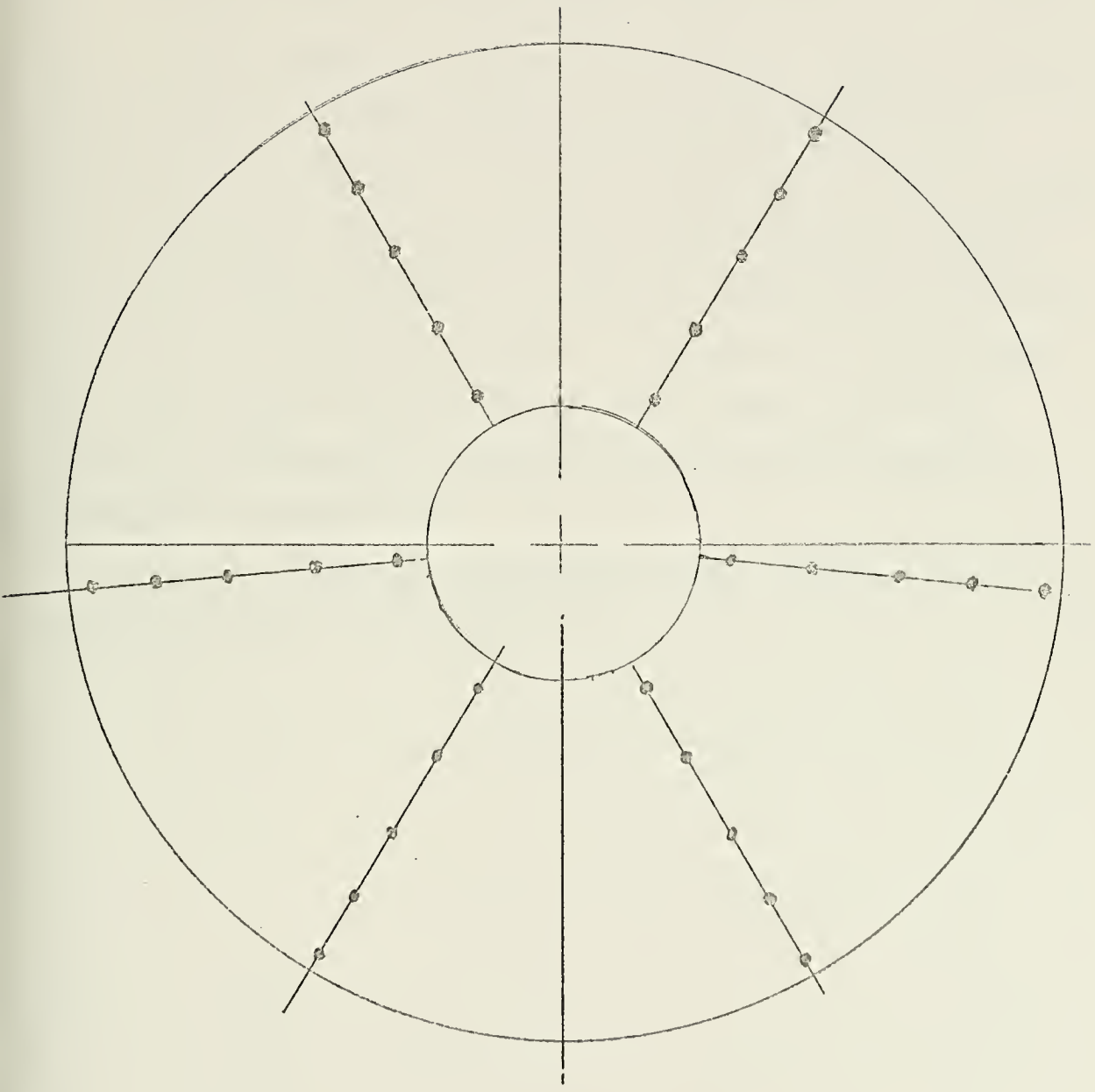

FIG. A-2 PLACEMENT OF PROBES

$$P_{REF} = P_{STEADY\text{-}STATE} - \Delta P_{AVG} \qquad \text{(A-1)}$$

$$P_{ABS} = P_{REF} + \text{Fluctuating Component} \qquad \text{(A-2)}$$

For each event the time of engine stall was known as well as the time of earliest indication of stall inside the compressor. This time of earliest indication of stall inside the compressor is the time at which the interstage dynamics indicated that the engine was going to stall and is accurate only to the nearest millisecond. A synopsis of these times for each stall event is in Table A-I. Also, a list of steady-state operating conditions for each stall event is contained in Table A-II.

If a more complete explanation of the instrumentation used is desired, consult Ref. 5.

TABLE A-1

STEADY-STATE OPERATING CONDITIONS

S. S. Rdg. No.	Dig. Tape Rdg. No.	M_o	P_o (psfa)	$\frac{\overline{P}_3}{\overline{P}_2}$	$\frac{Nx100}{\sqrt{T^*}}$	W_{corr} (lb/sec)	$\frac{\overline{P}_2}{P_o}$	$\frac{P_{rms}}{\overline{P}}_2$	(deg.)
154	01	2.50	1968.5	5.240	92.25	38.5	.799	.0691	0
162	02	2.58	1968.4	5.288	92.89	39.5	.769	.0460	5
141	03	2.50	1966.6	7.045	98.82	42.6	.761	.0851	0
148	04	2.50	1966.2	4.601	86.88	34.2	.788	.0658	0
164	05	2.58	1967.4	4.388	86.89	34.9	.843	.0185	5
82	06	2.58	1965.2	4.784	86.34	34.0	.854	.0156	5
103	07	2.68	1972.3	4.684	86.42	33.7	.736	.0500	0
200	08	2.50	1970.5	6.808	95.98	41.0	.768	.0275	0
214	09	2.50	1971.7	5.341	87.29	32.8	.739	.0209	0
219	10	2.50	1958.8	5.812	89.93	35.3	.794	.0167	0
261	11	2.58	1972.5	4.355	87.00	34.8	.783	.0209	6

TABLE A-2

TIMES OF INTEREST

Dig. Tape Rdg. No.	S. S. Rdg. No.	Digitizing Start days/hrs./mins./sec./ millisec.	Stop	Nominal t_{stall}	Earliest Indication of Stall Inside Compressor
01	154	234/00/38/47/291	47/541	47/506	47/493
02	162	234/02/02/35/073	35/323	35/288	35/281
03	141	233/04/23/40/362	40/612	40/577	40/575
04	148	233/05/34/16/722	16/972	16/937	16/932
05	164	234/02/33/17/851	18/101	18/066	18/056
06	82	226/01/39/11/926	12/176	12/141	12/135
07	103	227/02/09/16/045	16/295	16/260	16/253
08	200	235/02/04/00/640	00/890	00/855	00/853
09	214	235/03/30/19/734	19/984	19/949	
10	219	238/01/12/30/711	30/961	30/926	
11	261	239/02/52/28/583	28/833	28/798	28/789

Time code translation to month/day format of digitized tape:

day = 226;
month/day = 08/14

APPENDIX B

ACCURACY OF THE COMPUTER PROGRAM

When a computer program of this complexity is used, it is mandatory that the accuracy of the program be verified. In the calculation of the vorticity distribution at the compressor face there are six quantities involved: r', γ, normalized axial velocity, normalized total pressure, and the derivatives of the normalized pressure in the r' and theta directions. The distance r' is actually one of the defining values for any point on the compressor face, and gamma is merely the ratio of specific heats which is a well known function of temperature. The four remaining quantities are calculated by the program as a function of r' and θ that is provided by the interpolation scheme. Since the normalized axial velocity is a function of two measured quantities, the average total pressure and the average static pressure, and the total pressure, it is obvious that if the interpolation scheme accurately computes the total pressure at each point, then the normalized axial velocity also will be correct. Thus we see that the accuracy of the entire program hinges on the accuracy of the interpolation scheme which calculates p', $\frac{\partial p}{\partial r'}$, and $\frac{\partial p}{\partial \theta}$. The interpolation scheme is a cubic spline fit in two variables. It fits a cubic polynomial to each three points in one dimension and then matches the slope of the curve at the points that are common to both polynomials.

There are two ways to test the accuracy of this interpolation scheme. One way is to set up a dummy function of r' and θ, and produce a grid of point values of this dummy function. Then, using the interpolation scheme, predict the value of the dummy function and its two derivatives at other points in between the grid values and compare these values to the true values of the dummy function which are known since the dummy function is known explicitly. The second way is to plot the known values of the pressure on a graph, connect the points with a curve, and see if the interpolated values fall on the curve. The slope of the curve can be compared with the partial derivatives that were calculated. The results of the first method of testing are in Table B-1. In Figs. B-1 - B-5 the results of the second method are presented.

The interpolation scheme was found to have a maximum error of one percent for the value of pressure in this test, while the values of the partial derivatives were in error by a maximum of four percent.

Once the accuracy of the interpolation scheme has been verified, the only remaining possibility of error is the subroutines that print the map of the vorticity distribution. In Table B-II the values of vorticity calculated on a desk calculator are compared with the symbols that were printed at these points by the computer while drawing the maps. The positions of these points are indicated on the vorticity map in Fig. B-6.

TABLE B-I

PREDICTED VALUES OF A FUNCTION VS ACTUAL VALUES

Actual	Predicted	Actual	Predicted	Actual	Predicted
1918.2	1920.5	- 97.49	-100.3	45.66	43.59
1927.3	1929.4	-120.0	-122.9	141.5	144.6
1947.5	1950.0	-152.5	-156.1	268.6	271.0
1982.0	1984.9	-196.7	-201.1	426.8	431.7
2033.9	2036.8	-254.3	-259.6	616.2	617.6
2106.3	2111.3	-327.3	-355.0	836.8	856.6
1723.9	1723.0	-265.1	-265.2	-269.9	-267.5
1693.9	1693.3	-310.3	-309.6	-329.9	-331.9
1657.9	1657.1	-375.2	-374.8	-389.9	-391.1
1615.9	1614.9	-463.6	-463.2	-449.9	-452.2
1567.9	1566.8	-578.9	-578.1	-509.9	-511.6
1513.9	1512.1	-724.9	-726.5	-569.9	-576.3
1382.6	1382.1	-378.1	-378.7	-585.6	-574.4
1313.5	1314.2	-400.7	-401.0	-801.5	-802.1
1221.3	1222.0	-433.1	-433.7	-1048.6	-1044.5
1102.8	1103.8	-477.3	-478.1	-1326.8	-1324.4
954.9	956.9	-535.0	-535.7	-1636.2	-1625.8
774.5	774.9	-608.0	-610.1	-1976.8	-1990.0
941.8	941.3	-463.7	-463.1	-585.6	-574.4
872.7	873.4	-441.2	-440.9	-801.5	-802.1
780.5	781.2	-408.7	-408.2	-1048.6	-1044.5
661.9	662.9	-364.5	-363.8	-1326.8	-1324.4
514.1	516.0	-306.9	-306.1	-1636.2	-1625.8

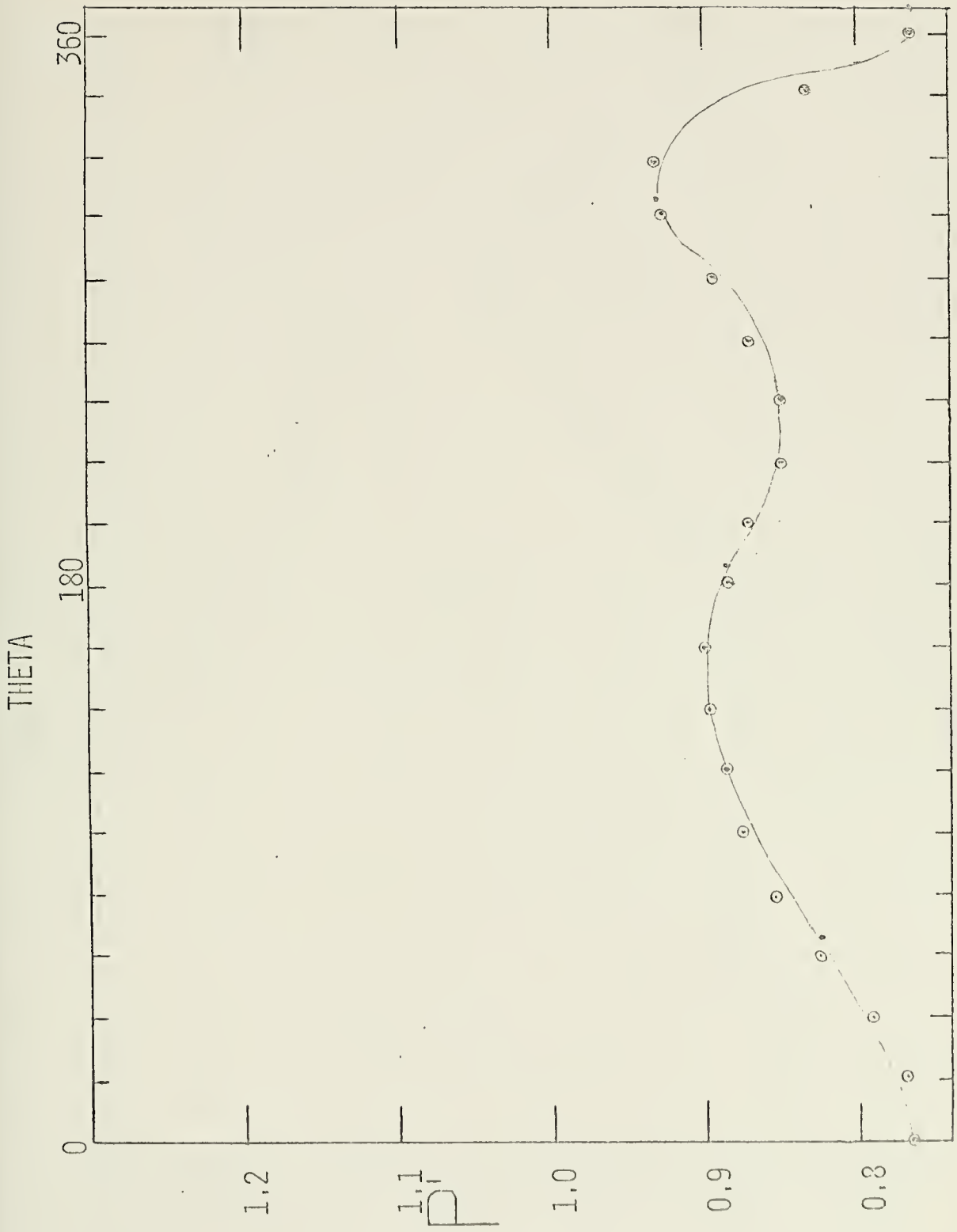

FIG. B-1 PRESSURE vs THETA, R'=0.41

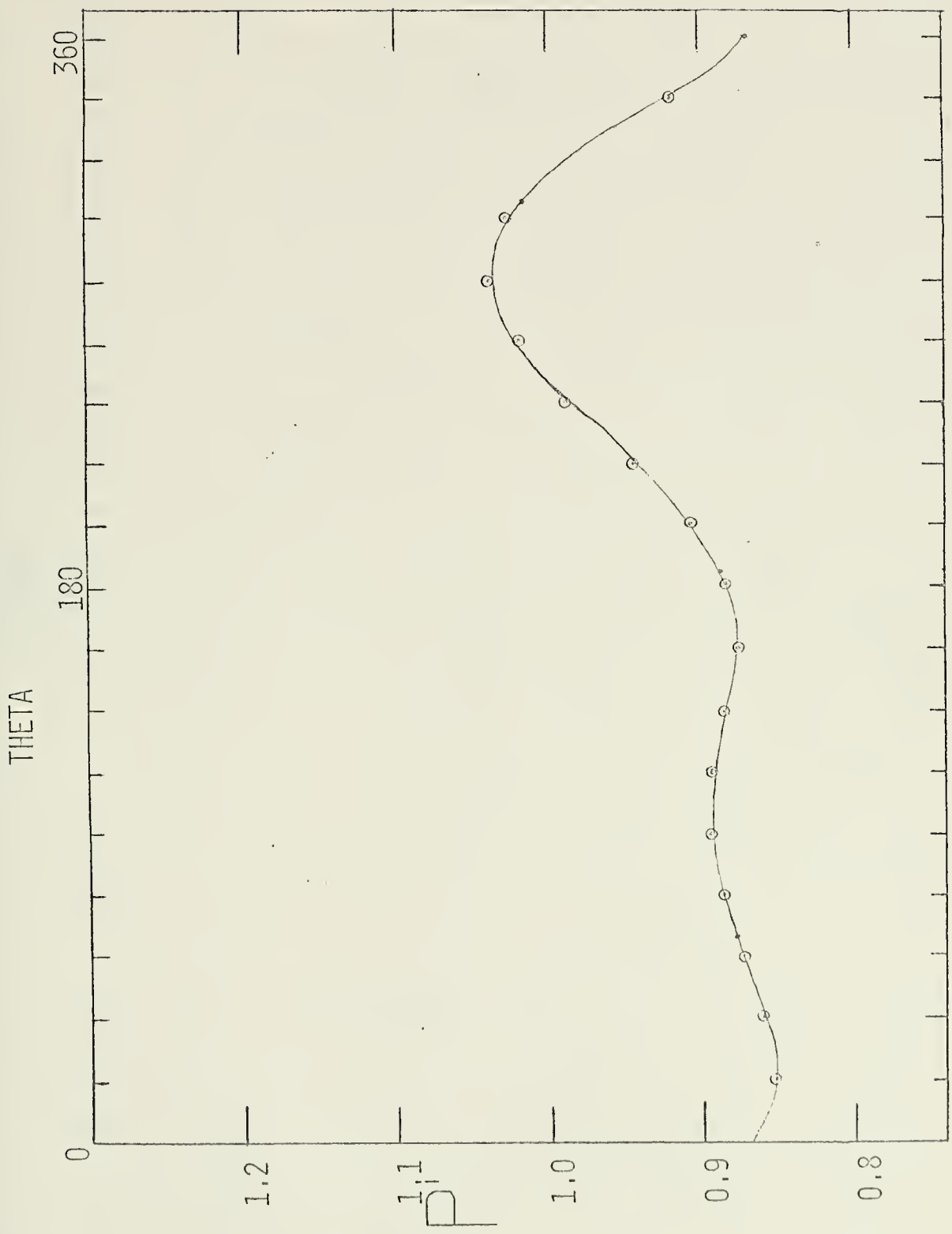

FIG. B-2 PRESSURE vs THETA, R'=0.59

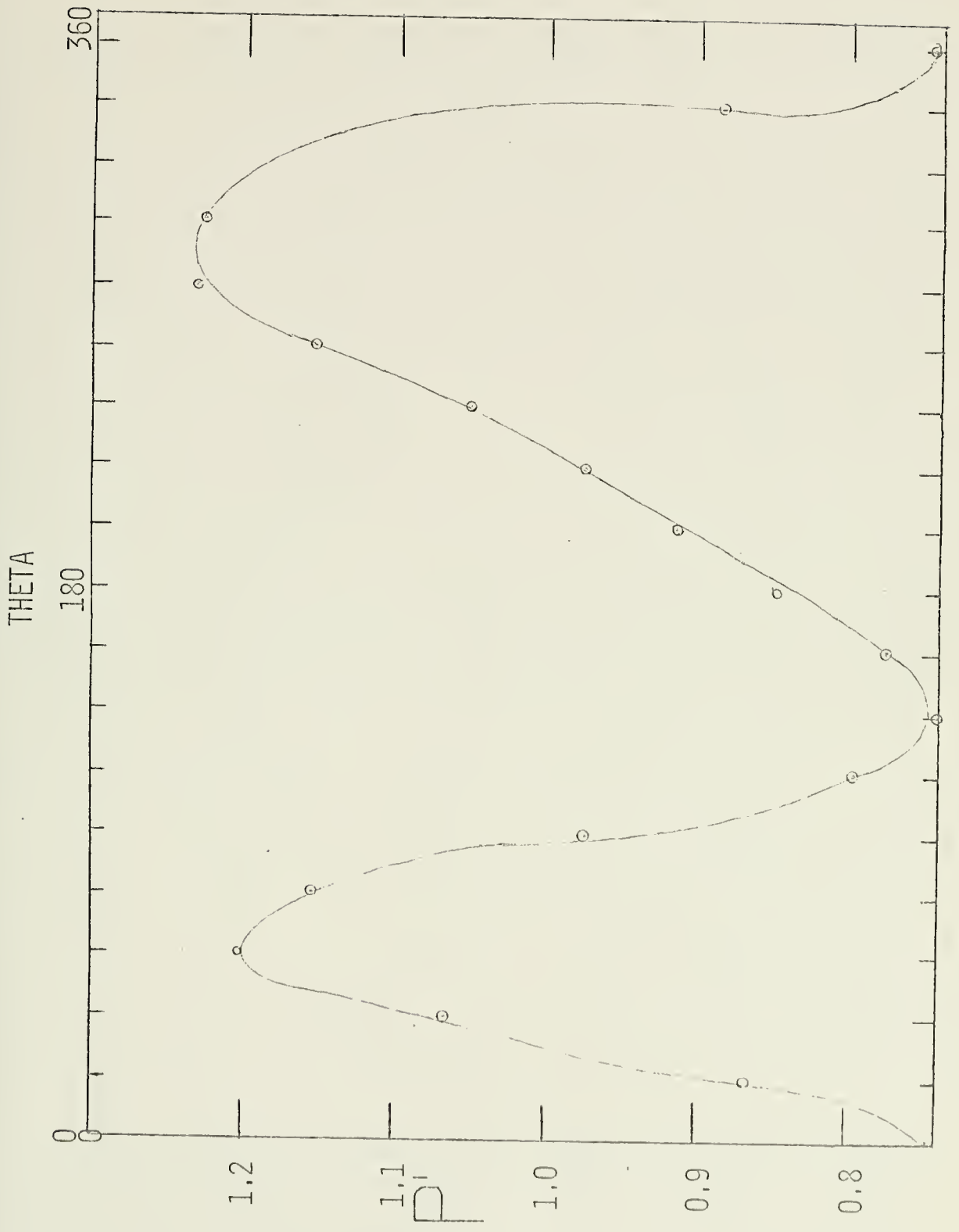

FIG. B-3 PRESSURE vs THETA, $R'=0.73$

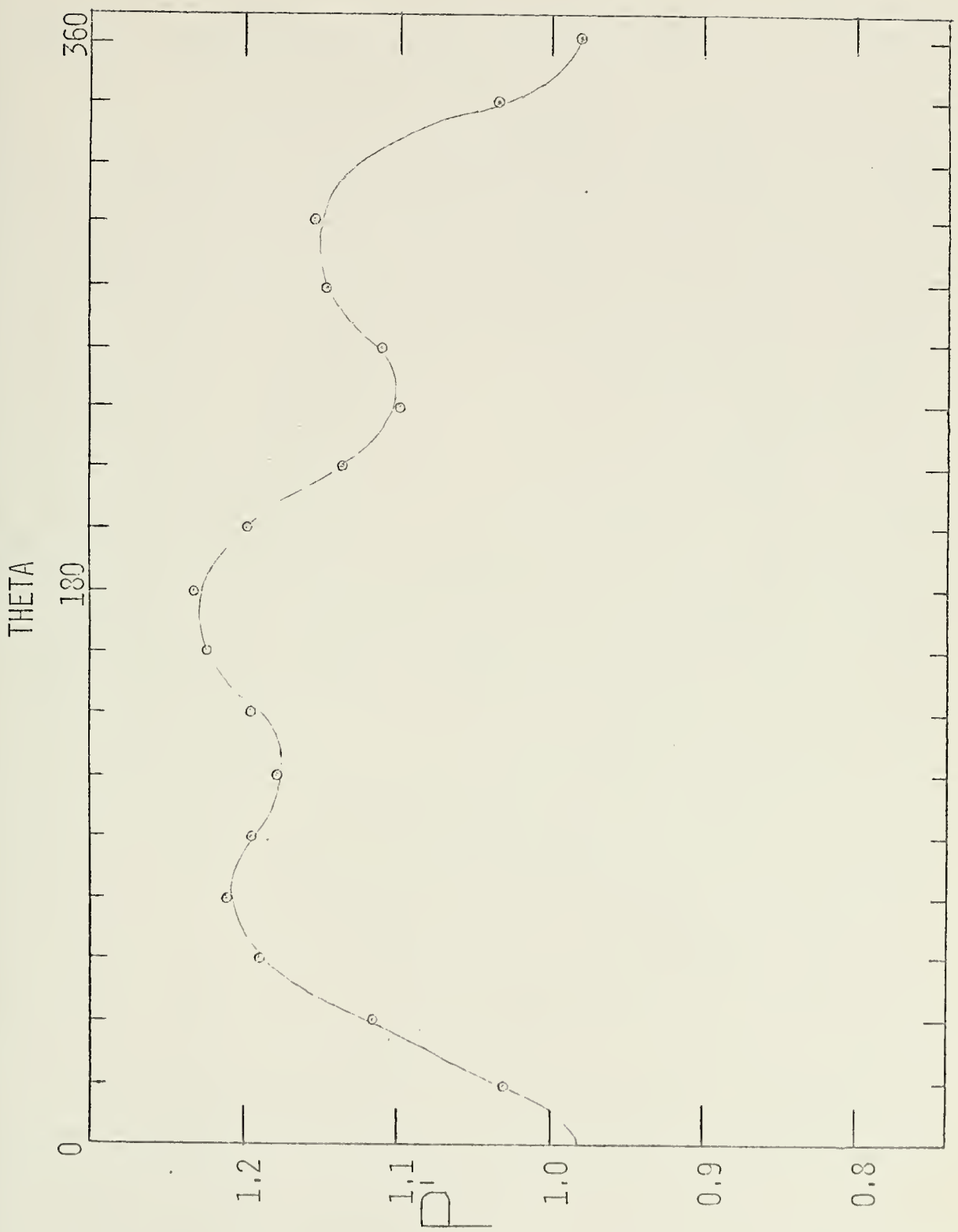

FIG. B-4 PRESSURE vs THETA, $R'=0.85$

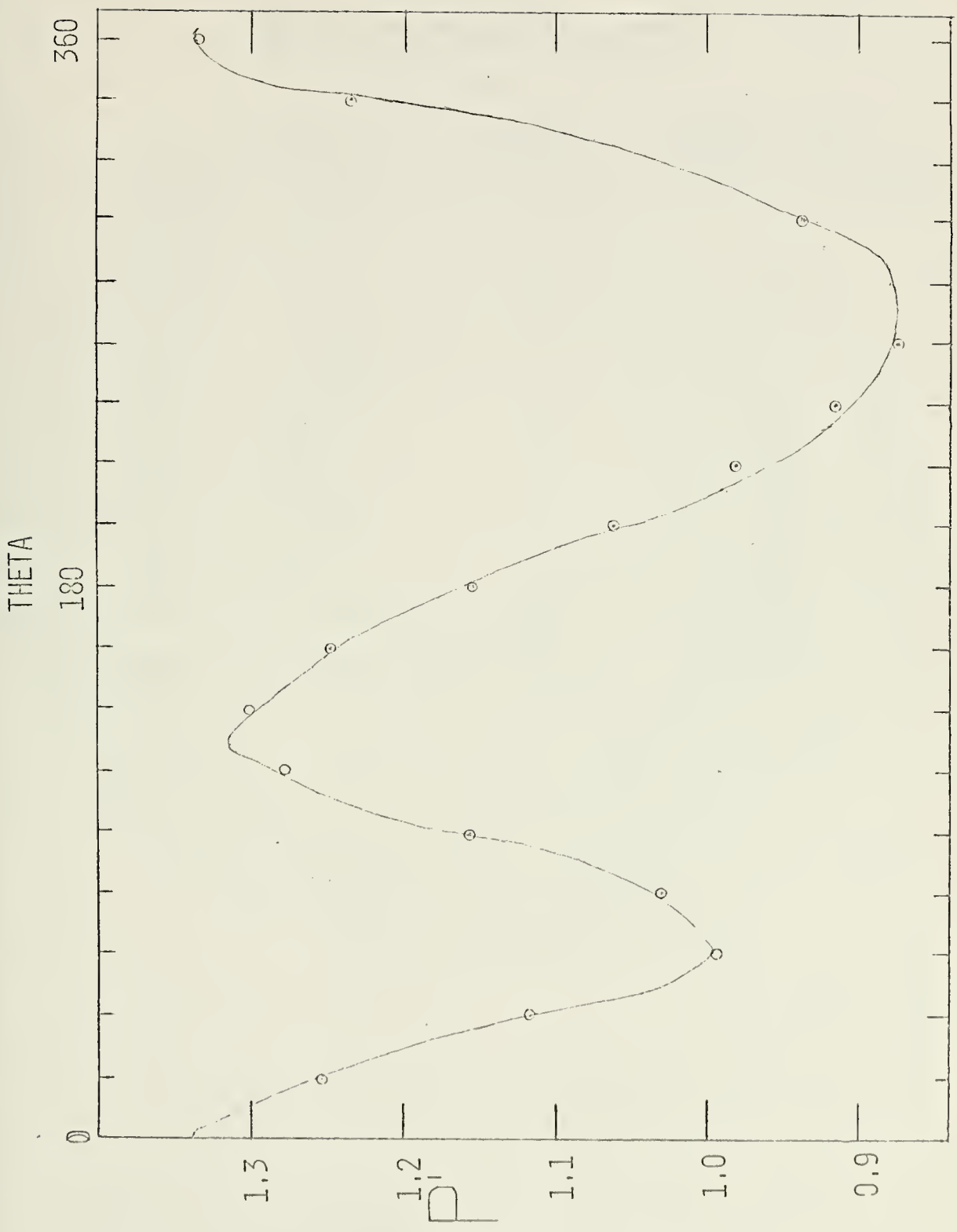

FIG. B-5 PRESSURE vs THETA, R'=0.95

TABLE B-II

TEST OF PRINT ROUTINE SYMBOLS

r'	θ	W'_θ	Symbol Printed	Symbol Which Should be Printed
.41	20°	1.055	-	-
.59	60°	-6.15	M	M
.73	100°	-1.09	K	K
.59	140°	.59954	*	*
.41	180°	-1.64	M	M
.85	180°	-1.89	M	M
.95	180°	-.1986	D	D
.73	180°	-2.1	M	M
.85	340°	-.296	D	D
.95	340°	.1657	O	O

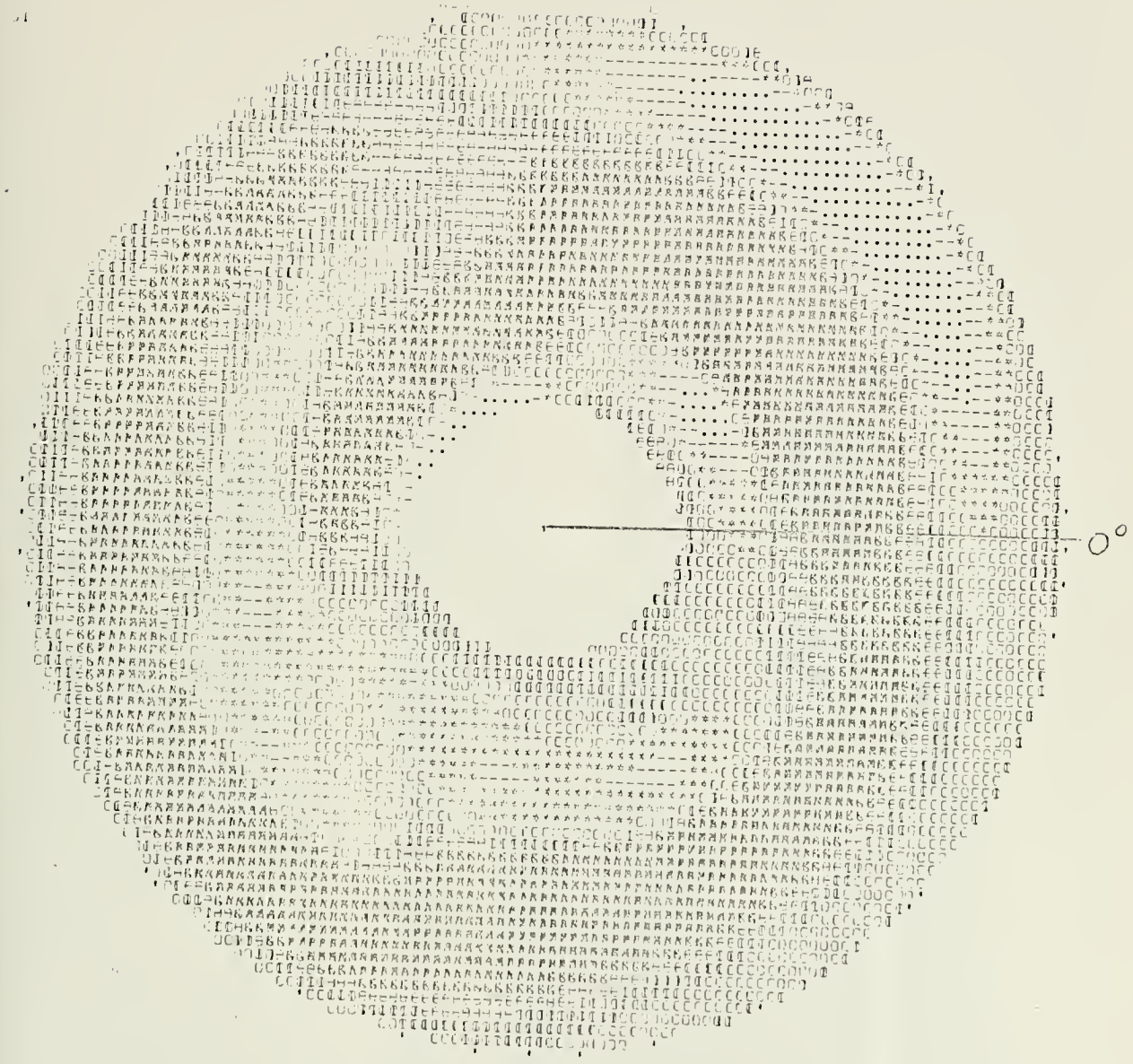

FIG. 3-6 MAP OF CIRCUMFERENTIAL VORTICITY

```
// EXEC FORTCLG,REGION.GO=250K
//FORT.SYSPRINT DD SYSOUT=O
//FORT.SYSIN DD *
C     ************************************************************
C
C       THIS PROGRAM IS DESIGNED TO TAKE THE DISTRIBUTIONS
C       OF TOTAL PRESSURE AT THE COMPRESSOR FACE AND FROM
C       THIS DATA CALCULATE THE DISTRIBUTION OF RADIAL
C       VORTICITY AND CIRCUMFERENTIAL VORTICITY AT THE FACE
C       OF THE COMPRESSOR.    THE INTERPOLATION SCHEME
C       USED  WAS DEVELOPED AT THE LEWIS RESEARCH CENTER OF
C       NASA.    THE PART OF THE PROGRAM THAT  PRINTS A MAP
C       OF VALUES OVER THE COMPRESSOR FACE WAS DEVELOPED
C       AT WRIGHT PATTERSON AIR FORCE BASE AND ALTERED AT
C       THE NAVAL POSTGRADUATE SCHOOL IN MONTEREY CALIFORNIA
C
C     ************************************************************
      INTEGER*2 TAPED,MCOUNT,CAL,A
      INTEGER*2 INTRIM
C
C     THESE COMMON BLOCKS ARE THE INTERFACE BETWEEN
C     THE MAIN PROGRAM AND THE PRINT ROUTINE OF SUBPROGRAMS
C     THEY ELIMINATE THE NEED FOR USING ALL OF THE VARIABLES
C     NEEDED BY A PROGRAM WHEN CALLING FROM THE MAIN PROGRAM
C
      COMMON/PDATA/RAD(10),ANG(20),CHART(10,20),NAI,NRI,RH,RT
      COMMON/LEGND/CPR(10),DPR(10),PLO,DELP,NPR
      COMMON/RAP/TITLE(48),ICASE
      DIMENSION TITLEX(48),TITLE2(48),TITLE3(48)
      DIMENSION ANGLE(20)
      DIMENSION THETA(20),PVORT(20,10),DPDTH(20,10),DPDR(20,10),
     1PCVORT(20,10),VORTRA(20,10),UZVORT(20,10),VORT(20,10)
      DIMENSION  HETA(10),PT(10,10),PP(10,10),RP(10),THETAO(10)
      DIMENSION CPRX(10),DPRX(10)
      DIMENSION PO(10,10),PCP(10,10),MCOUNT(10,10),DELTAP(10,10)
      DIMENSION TAPED(960)
      DIMENSION INTRIM(32,30)
C
C     THIS INPUT DATA CONTAINS THE GEOMETRY OF THE PRESSURE
C     PROBES AS WELL AS MOST OF THE DATA NEEDED BY THE PRINT
C     SUBPROGRAMS. DPRX AND CPRX ARE THE SYMBOLS USED BY
C     THE  SHAY SUBPROGRAM THE DRAW THE MAP OF THE COMPRESSOR
C     FACE.
C
      DATA DPRX/1HM,1HK,1H-,1HI,1H ,1H ,1H ,1H /
      DATA CPRX/1HA,1HG,1HC,1HO,1HO,1H*,1H-,1H./
      DATA PLOX,DELX,NPRX/-1.5,.5,7/
      DELPX=DELX
```

```
      DATA NAIX,NRIX,RHX,RTX/18,7,.27531,1.0/
      DATA ICAS /1234/
      ICASE=ICAS
      DATA RP/.27531,.41014,.59419,.73342,.85014,.95267,.99999/
      DATA GAMMA/1.4/
      DATA NR/7/
      DATA THETAO/-55.,0.,65.,120.,185.,240.,305.,360.,425./
      DATA NT/9/
      DATA PI/3.14157/
      DATA THETA/0.,20.,40.,60.,80.,100.,120.,140.,160.,180.,
     A200.,220.,240.,260.,280.,300.,340.,360. /
      DATA NRUN/4/
      DATA PSTATC/1306.14/
      NRUNS=(NRUN+3)*64+52
      NMAP=1307
      NRUNS=NRUNS-5
      DO 27 N=1,NRUNS
      READ(4,105) TAPED
   27 CONTINUE
      B=72.0*10.0/3094.0
      CAL=4096
      READ(5,110)(TITLE(I),I=1,48)
      READ(5,110)(TITLE2(I),I=1,48)
      READ(5,110)(TITLE3(I),I=1,48)
      DO 17 N=1,9
   17 THETAO(N)=THETAO(N)*PI/180.0
      DO 75 N=1,NAIX
      ANGLE(N)=THETA(N)
      THETA(N)=THETA(N)*PI/180.0
   75 CONTINUE
      DO 952 N=1,48
  952 TITLEX(N)=TITLE(N)
C
CCC   THE VALUES OF STATIC PRESSURE AT EACH OF THE PROBES
CCC   ARE READ IN HERE
C
      DO 1 N=2,7
    1 READ(5,103)(PO(N,J),J=1,7)
C
CCC   THE VALUES OF THE PRESSURES AT AN ANGLE OF 360 ARE
CCC    SET EQUAL TO THE PRESSURES AT AN ANGLE OF0
CCC   IN ORDER TO ASSURE THAT THE INTERPOLATION SCHEME
CCC   WILL BE SMOOTH
C
      DO 50 J=1,7
      PO(9,J)=PO(3,J)
      PO(1,J)=PO(7,J)
   50 PO(8,J)=PO(2,J)
```

```
      PSUM=0.0 D00
      DC 2 N=2,7
      DC 2 J=2,6
    2 PSUM=PSUM+PO(N,J)
      PAVE=PSUM/30.0D 00
      DC 65 I=1,9
      DC 65 J=1,7
      PCP(I,J)=PC(I,J)/PAVE
   65 CONTINUE
C
C      STATEMENT 100 US A SWITCHING POINT THAT CAN BE RETURNED TO
C     IN ORDER TO CALCULATE VALUES OF VORTICITY FOR THE SAME
C     STATIC PRESSURES BUT DIFFERENT DYNAMIC PRESSURES
C     USED IN THE CALCULATION OF VORTICITY
C
  100 CONTINUE
      NMAP=NMAP+2
      READ(4,105) TAPED
      DC 600 N=1,32
      JUST=(N-1)*30+1
      JEST=JUST+29
      DC 600 J=JUST,JEST
      KLAP=J-JUST+1
      INTRIM(N,KLAP)=TAPED(J)
  600 CONTINUE
      NCASE=1
  700 DC 605 N=2,7
      JUST=(N-2)*5+1
      JEST=JUST+4
      DC 605 J=JUST,JEST
      KLAP=J-JUST+2
      MCOUNT(N,KLAP)=INTRIM(NCASE,J)
  605 CONTINUE
      NCASE=NCASE+5
      DC 55 I=1,10
      CPR(I)=CPRX(I)
      DPR(I)=DPRX(I)
   55 CONTINUE
      PLC=0.
      DELP=0.
      MAI=MAIX
      NRI=NRIX
      RF=RHX
      RT=RTX
      NPR=NPRX
      WRITE(6,213) NRUN,NMAP
      WRITE(6,209)
      ICASE=NMAP
```

```
      DO 500 I=2,7
  500 WRITE(6,210)(MCOUNT(I,J),J=2,6)
      PTSUM=0.0
      DO 4 I=2,7
      DO 4 J=2,6
      A=MCOUNT(I,J)-CAL
      DELTAP(I,J)=A*B
      PT(I,J)=PO(I,J)+DELTAP(I,J)
    4 CONTINUE
      DELTAP(8,2)=DELTAP(2,2)
      DELTAP(8,6)=DELTAP(2,6)
      DO 53 I=2,8
      PT(I,7)=PO(I,7)+DELTAP(I,6)
      PT(I,1)=PO(I,1)+DELTAP(I,2)
   53 CONTINUE
      DO 51 J=1,7
      PT(9,J)=PT(3,J)
      PT(1,J)=PT(7,J)
   51 PT(8,J)=PT(2,J)
      DO 5 I=2,7
      DO 5 J=2,6
    5 PTSUM=PTSUM+PT(I,J)
      PTAVE=PTSUM/30.0D 00
      XMACHP=UZMACH(PTAVE,PSTATC)
      DO 6 I=1,9
      DO 6 J=1,7
    6 PP(I,J)=PT(I,J)/PTAVE
      WRITE(6,204)
      WRITE(6,205) (THETAC(I),I=2,8)
      DO 45 J=1,7
      WRITE(6,206) RP(J),(PT(I,J),I=2,8)
      WRITE(6,206) RP(J),(PP(I,J),I=2,8)
   45 CONTINUE
      EXTERNAL SPLIN2,SPLIN1,F2,FX,FY
      CALL SPLIN2(THETAC,RP,PP,NT,NR)
      DO 80 N=1,NAIX
      ANG(N)=ANGLE(N)
   80 CONTINUE
      DO 81 N=1,7
      RAD(N)=RP(N)
   81 CONTINUE
      DO 82 I=1,NAIX
      DO 82 J=1,NRIX
      X=THETA(I)
      Y=RAD(J)
      PVORT(I,J)=F2(X,Y)
      DPDTH(I,J)=FX(X,Y)
      DPDR(I,J)=FY(X,Y)
```

```
   82 CONTINUE
      WRITE(6,207)
      DO 76 I=1,NAIX
   76 WRITE(6,208)(PVORT(I,J),J=1,7)
      WRITE (6,211)
      DO 501 I=1,NAIX
  501 WRITE(6,208)(DPDR(I,J),J=1,7)
      WRITE(6,212)
      DO 502 I=1,NAIX
  502 WRITE(6,208) (DPDTH(I,J),J=1,7)
      DO 85 I=1,NAIX
      DO 85 J=1,NRIX
      PTSUB=PVORT(I,J)*PTAVE
      UZVORT(I,J)=UZPRIM(XMACHP,PTSUB,PSTATC,PTAVE)
   85 CONTINUE
      DO 86 I=1,NAIX
      DO 86 J=1,NRIX
      VORT(I,J)=(-1./(GAMMA*PVORT(I,J)*UZVORT(I,J)))*DPDR(I,J)
      VORTRA(I,J)=DPDTH(I,J)/(GAMMA*PVORT(I,J)*UZVORT(I,J)*RP(J))
   86 CONTINUE
      WRITE(6,201)
      WRITE(6,203) PTAVE
      DO 90 I=1,NAIX
      DO 90 J=1,NRIX
   90 CHART(J,I)=PVORT(I,J)
C
C     THE FOLLOWING SEQUENCE OF STATEMENTS WILL CAUSE
C     A MAP OF TOTAL PRESSURE ON THE COMPRESSOR FACE
C     TO BE PRINTED OUT
      DO 953 N=1,48
  953 TITLE(N)=TITLEX(N)
C
      CALL CFACE(IX,IY,5)
      CALL SHADY
      DO 56 I=1,10
      CPR(I)=CPRX(I)
   56 DPR(I)=DPRX(I)
      PLO=PLOX
      DELP=DELPX
      NAI=NAIX
      NRI=NRIX
      RH=RHX
      RT=RTX
      NPR=NPRX
      DO 57 I=1,NAIX
   57 ANG(I)=ANGLE(I)
      DO 58 I=1,7
   58 RAD(I)=RP(I)
```

```
      DO 91 I=1,NAIX
      DO 91 J=1,NRIX
      CHART(J,I)=VORT(I,J)
   91 CONTINUE
      WRITE(6,202)
C
      DO 950 N=1,48
  950 TITLE(N)=TITLE2(N)
C     THE FOLLWING SEQUENCE OF STATEMENTS WILL CAUSE
C     A MAP OF VORTICITY ON THE COMPRESSOR FACE TO BE PRINTED
C
      CALL CFACE(IX,IY,5)
      CALL SHADY
      DO 92 I=1,10
      CPR(I)=CPRX(I)
   92 DPR(I)=DPRX(I)
      PLC=PLOX
      NAI=NAIX
      NRI=NRIX
      RH=RHX
      RT=RTX
      NPR=NPRX
      DO 93 I=1,NAIX
   93 ANG(I)=ANGLE(I)
      DO 94 I=1,NRIX
   94 RAD(I)=RP(I)
      DO 95 J=1,NAIX
      DO 95 J=1,NRIX
      CHART(J,I)=VORTRA(I,J)
   95 CONTINUE
      DO 951 N=1,48
  951 TITLE(N)=TITLE3(N)
      CALL CFACE(IX,IY,5)
      CALL SHADY
      IF (NCASE.GT. 32) GO TO 100
      NMAP=NMAP+5
      GO TO 700
  103 FORMAT(7F10.4)
  104 FORMAT(I4,1X,I4,1X,I4,1X,I4,1X,I4)
  105 FORMAT(4(20A2),16OA2)
  110 FORMAT(48A1)
  201 FORMAT(//,15X,' THIS IS A MAP OF PRESSURE'//)
  202 FORMAT(//,15X,'THIS IS A MAP OF VORTICITY',//)
  203 FORMAT(//,5X,'THE AVERAGE TOTAL PRESSURE IS',F12.5)
  204 FORMAT(//,15X,'THIS IS A TABLE OF PT AND PPRIME',///)
  205 FORMAT(///,15X,7F11.5)
  206 FORMAT(/,5X,F10.4,7E11.4)
  207 FORMAT(///,15X,'THIS IS A TABLE OF PPRIME INTERPOLATED'///)
```

```
  208 FORMAT(/,25X,7F10.4)
  209 FORMAT(//,40X,'***INPUT CHECK***',//)
  210 FORMAT(/,15X,5I10)
  211 FORMAT(///,15X,'THIS IS A TABLE OF DP/DR')
  212 FORMAT(///,15X,'THIS IS A TABLE OF DP/DTHETA')
  213 FORMAT(//,15X,'****FOR RUN NUMBER',1X,I2,2X,'CASE NUMBER',1X,I4,'*
     1***',///)
      STOP
      END


      FUNCTION UZMACH(PTF,POF)
C
CC    THIS SUBROUTINE CALCULATES THE AXIAL MACH NUMBER
C
      G=1.4
      A=(G-1.0)/G
      B=2.0/(G-1.0)
      C=PTF/POF
      IF(C.LT.0.) C=-C
      UZMACH=B*((C**A)-1.0)
      UZMACH=SQRT(UZMACH)
      RETURN
      END


      FUNCTION UZPRIM(XM,PTF,POFA,PTFA)
C     THIS  SUBPROGRAM CALCULATES THE AXIAL VELOCITY TO BE
      A=PTFA-POFA
      B=(PTF-POFA)/A
      IF (B.LE. 0.0) GO TO 59
      C=SQRT(B)
      UZPRIM=XM*C
      RETURN
   59 UZPRIM=1.0
      RETURN
      END


      SUBROUTINE SPLIN2(X,Y,Z,N,M)
      DIMENSION X(20),Y(20),Z(10,10),ZI(20),ZP(20)
      COMMON/SPLIN/N1,M1,X1(20),Y1(20),ZI(10,10),ZX(10,10),ZY(10,10),
     1 ZYX(10,10)
      COMMON /BNDRY/ BX1(20),BXN(20),JX,BY1(20),BYM(20),JY                    5
      N1 = N                                                                  6
      M1 = M                                                                  7
      DO 10 I=1,N1                                                            8
   10 X1(I) = X(I)                                                            9
```

```
      DO 11 J=1,M1                                                      10
   11 Y1(J) = Y(J)                                                      11
      DO 12 I=1,N1                                                      12
      DO 12 J=1,M1                                                      13
   12 Z1(I,J) = Z(I,J)                                                  14
      DO 3 I=1,N1                                                       15
      DO 1 J=1,M1                                                       16
    1 ZI(J) = Z1(I,J)                                                   17
      CALL SPLIN1(Y1,ZI,M1,ZP,BY1(I),BYM(I),JY)                         18
      DO 2 J=1,M1                                                       19
    2 ZY(I,J) = ZP(J)                                                   20
    3 CONTINUE                                                          21
      DO 6 J=1,M1                                                       22
      DO 4 I=1,N1                                                       23
    4 ZI(I) = Z1(I,J)                                                   24
      CALL SPLIN1(X1,ZI,N1,ZP,BX1(J),BXN(J),JX)                         25
      DO 5 I=1,N1                                                       26
    5 ZX(I,J) = ZP(I)                                                   27
    6 CONTINUE                                                          28
      DO 9 J=1,M1                                                       29
      DO 7 I=1,N1                                                       30
    7 ZI(I) = ZY(I,J)                                                   31
      CALL SPLIN1(X1,ZI,N1,ZP,0.0,0.0,2)                                32
      DO 8 I=1,N1                                                       33
    8 ZYX(I,J) = ZP(I)                                                  34
    9 CONTINUE                                                          35
      RETURN                                                            36
      END                                                               37

      BLOCK DATA                                                         1
      COMMON /BNDRY/ BX1(20),BXN(20),JX,BY1(20),BYM(20),JY               2
      DATA BX1,BXN,BY1,BYM,JX,JY/80*0.0,2*2/                             3
      END                                                                4

      SUBROUTINE SPLIN1(X,Y,N,DY,B1,BN,J)
      DIMENSION X(1),Y(1),DY(1),A(20),B(20),C(20),D(20)                  2
      N1 = N-1                                                           3
      GO TO (4,5),J                                                      4
    4 B(1) = 1.0                                                         5
      C(1) = 0.0                                                         6
      D(1) = B1                                                          7
      A(N) = 0.0                                                         8
      B(N) = 1.0                                                         9
      D(N) = BN                                                         10
      GO TO 6                                                           11
    5 B(1) = 2.0                                                        12
```

```
      C(1) = 1.0                                                                13
      D(1) = 3.0*(Y(2)-Y(1))/(X(2)-X(1))-0.5*(X(2)-X(1))*B1                     14
      A(N) = 1.0                                                                15
      B(N) = 2.0                                                                16
      D(N) = 3.0*(Y(N)-Y(N1))/(X(N)-X(N1))+0.5*(X(N)-X(N1))*BN                  17
    6 DO 1 I=2,N1                                                               18
      A(I) = X(I+1)-X(I)                                                        19
      B(I) = 2.0*(X(I+1)-X(I-1))                                                20
      C(I) = X(I)-X(I-1)                                                        21
    1 D(I) = 3.0*(Y(I+1)*C(I)**2+Y(I)*(A(I)**2-C(I)**2)-Y(I-1)*A(I)**2)/        22
     *(C(I)*A(I))                                                               23
      D(1) = D(1)/B(1)                                                          24
      DO 2 I=2,N                                                                25
      B(I) = B(I)-A(I)*C(I-1)/B(I-1)                                            26
    2 D(I) = (D(I)-A(I)*D(I-1))/B(I)                                            27
      DY(N) = D(N)                                                              28
      DO 3 I=1,N1                                                               29
      K = N-I                                                                   30
    3 DY(K) = D(K)-C(K)*DY(K+1)/B(K)                                            31
      RETURN                                                                    32
      END                                                                       33


      FUNCTION F2(X1,Y1)
      COMMON/SPLIN/N,M,X(20),Y(20),Z(10,10),ZX(10,10),ZY(10,10),
     1 ZYX(10,10)
      G(FI,FI1,DFI,DFI1,DEL,S) = (2.0*(FI-FI1)+DEL*(DFI+DFI1))*(S/DEL)**        4
     * 3 + (3.0*(FI1-FI)-DEL*(2.0*DFI+DFI1))*(S/DEL)**2 + DFI*S + FI            5
      IF(X1.LT.X(1))  WRITE (6,201)
      DO 1 I=2,N                                                                7
      K = I-1                                                                   8
      IF(X1.LE.X(I))  GO TO 2                                                   9
    1 CONTINUE                                                                 10
      WRITE (6,202)
    2 IF(Y1.LT.Y(1))  WRITE (6,203)
      DO 3 J=2,M                                                               13
      L = J-1                                                                  14
      IF(Y1.LE.Y(J))  GO TO 4                                                  15
    3 CONTINUE                                                                 16
      WRITE (6,204)
    4 DEL = X(K+1)-X(K)                                                        18
      S = X1-X(K)                                                              19
      FXJ = G(Z(K,L),Z(K+1,L),ZX(K,L),ZX(K+1,L),DEL,S)                         20
      FXJ1 = G(Z(K,L+1),Z(K+1,L+1),ZX(K,L+1),ZX(K+1,L+1),DEL,S)                21
      FYXJ = G(ZY(K,L),ZY(K+1,L),ZYX(K,L),ZYX(K+1,L),DEL,S)                    22
      FYXJ1 = G(ZY(K,L+1),ZY(K+1,L+1),ZYX(K,L+1),ZYX(K+1,L+1),DEL,S)           23
      DEL = Y(L+1)-Y(L)                                                        24
      S = Y1-Y(L)                                                              25
```

```
      F2= G(FXJ,FXJ1,FYXJ,FYXJ1,DEL,S)                                  26
      RETURN                                                            27
  201 FORMAT (' **WARNING** X BELOW XMIN IN F2')
  202 FORMAT (' **WARNING** X ABOVE XMAX IN F2')
  203 FORMAT (' **WARNING** Y BELOW YMIN IN F2')
  204 FORMAT (' **WARNING** Y ABOVE YMAX IN F2')
      END                                                               28


      FUNCTION FX(X1,Y1)
      COMMON/SPLIN/N,M,X(20),Y(20),Z(10,10),ZX(10,10),ZY(10,10),
     1 ZYX(10,10)
      G(FI,FI1,DFI,DFI1,DEL,S) = (2.0*(FI-FI1)+DEL*(DFI+DFI1))*(S/DEL)**  4
     * 3 + (3.0*(FI1-FI)-DEL*(2.0*DFI+DFI1))*(S/DEL)**2 + DFI*S + FI      5
      DG(FI,FI1,DFI,DFI1,DEL,S) = (6.0*(FI-FI1)+3.0*DEL*(DFI+DFI1))*     6
     *  (S**2/DEL**3)+(6.0*(FI1-FI)-2.0*DEL*(2.0*DFI+DFI1))*(S/DEL**2)+  7
     * DFI                                                                8
      IF(X1.LT.X(1))  WRITE (6,201)
      DO 1 I=2,N                                                        10
      K = I-1                                                           11
      IF(X1.LE.X(I))  GO TO 2                                           12
    1 CONTINUE                                                          13
      WRITE (6,202)
    2 IF(Y1.LT.Y(1))  WRITE (6,203)
      DO 3 J=2,M                                                        16
      L = J-1                                                           17
      IF(Y1.LE.Y(J))  GO TO 4                                           18
    3 CONTINUE                                                          19
      WRITE (6,204)
    4 DEL = X(K+1)-X(K)                                                 21
      S = X1-X(K)                                                       22
      FXJ =DG(Z(K,L),Z(K+1,L),ZX(K,L),ZX(K+1,L),DEL,S)                  23
      FXJ1 =DG(Z(K,L+1),Z(K+1,L+1),ZX(K,L+1),ZX(K+1,L+1),DEL,S)         24
      FYXJ =DG(ZY(K,L),ZY(K+1,L),ZYX(K,L),ZYX(K+1,L),DEL,S)             25
      FYXJ1 =DG(ZY(K,L+1),ZY(K+1,L+1),ZYX(K,L+1),ZYX(K+1,L+1),DEL,S)    26
      DEL = Y(L+1)-Y(L)                                                 27
      S = Y1-Y(L)                                                       28
      FX =G(FXJ,FXJ1,FYXJ,FYXJ1,DEL,S)                                  29
      RETURN                                                            30
  201 FORMAT (' **WARNING** X BELOW XMIN IN FX')
  202 FORMAT (' **WARNING** X ABOVE XMAX IN FX')
  203 FORMAT (' **WARNING** Y BELOW YMIN IN FX')
  204 FORMAT (' **WARNING** Y ABOVE YMAX IN FX')
      END                                                               31
```

```
      FUNCTION FY(X1,Y1)
      COMMON/SPLIN/N,M,X(20),Y(20),Z(10,10),ZX(10,10),ZY(10,10),
     1 ZYX(10,10)
      G(FI,FI1,DFI,DFI1,DEL,S) = (2.0*(FI-FI1)+DEL*(DFI+DFI1))*(S/DEL)**
     * 3 + (3.0*(FI1-FI)-DEL*(2.0*DFI+DFI1))*(S/DEL)**2 + DFI*S + FI
      DG(FI,FI1,DFI,DFI1,DEL,S) = (6.0*(FI-FI1)+3.0*DEL*(DFI+DFI1))*
     * (S**2/DEL**3)+(6.0*(FI1-FI)-2.0*DEL*(2.0*DFI+DFI1))*(S/DEL**2)+
     * DFI
      IF(X1.LT.X(1))  WRITE (6,201)
      DO 1 I=2,N
      K = I-1
      IF(X1.LE.X(I))  GO TO 2
    1 CONTINUE
      WRITE (6,202)
    2 IF(Y1.LT.Y(1))  WRITE (6,203)
      DO 3 J=2,M
      L = J-1
      IF(Y1.LE.Y(J))  GO TO 4
    3 CONTINUE
      WRITE (6,204)
    4 DEL = X(K+1)-X(K)
      S = X1-X(K)
      FXJ = G(Z(K,L),Z(K+1,L),ZX(K,L),ZX(K+1,L),DEL,S)
      FXJ1 = G(Z(K,L+1),Z(K+1,L+1),ZX(K,L+1),ZX(K+1,L+1),DEL,S)
      FYXJ = G(ZY(K,L),ZY(K+1,L),ZYX(K,L),ZYX(K+1,L),DEL,S)
      FYXJ1 = G(ZY(K,L+1),ZY(K+1,L+1),ZYX(K,L+1),ZYX(K+1,L+1),DEL,S)
      DEL = Y(L+1)-Y(L)
      S = Y1-Y(L)
      FY =DG(FXJ,FXJ1,FYXJ,FYXJ1,DEL,S)
      RETURN
  201 FORMAT (' **WARNING** X BELOW XMIN IN FY')
  202 FORMAT (' **WARNING** X ABOVE XMAX IN FY')
  203 FORMAT (' **WARNING** Y BELOW YMIN IN FY')
  204 FORMAT (' **WARNING** Y ABOVE YMAX IN FY')
      END


      SUBROUTINE CFACE(IX,IY,IQ)
      COMMON /LEGND/ CPR(10), DPR(10),PLC,DELP,NPR
      COMMON /PAGE/C(81,101), D(81,101)
      DIMENSION THT(40,50), RHO(40,50)
      DATA PI/3.14159/
      GO TO (10,20,30,40,60,70),IQ
C
C     INITIALIZATION
60    DO 2 I=1,50
      RHO(1,I) = FLOAT(I-1)/50.
      THT(1,I) = 0.
```

```
      IF(I .GT. 40) GO TO 2
      RHO(I,1) = FLOAT(I-1)/40.
      THT(I,1) = 90.
2     CONTINUE
      DO 1 I=2,40
      DO 1 J=2,50
      X = FLOAT(J-1)/50.
      Y = FLOAT(I-1)/40.
      R = SQRT(X*X+Y*Y)
      THETA=ATAN(Y/X)*180./PI
      RHO(I,J) = R
      THT(I,J) = THETA
1     CONTINUE
      RETURN
   70 WRITE(6,200)
  200 FORMAT(1H1,//,11X,6HLEGEND,///)
      WRITE(6,203) CPR(8)
      WRITE(6,202) DPR(8)
201   FORMAT(1H ,7XF6.2//)
202   FORMAT(1H+,16XA1//)
203   FORMAT(1H ,16XA1)
      XLEGND = PLC+DELP*FLOAT(NPR-1)
      DO 17 I=1,NPR
      K = NPR+1-I
      WRITE(6,201) XLEGND
      WRITE(6,203) CPR(K)
      WRITE(6,202) DPR(K)
17    XLEGND = XLEGND-DELP
      RETURN
C
C     1ST QUADRANT
10    IF(IX .EQ. 1) RETURN
      R = RHO(IY,IX)
      THETA = THT(IY,IX)
      JX = IX+50
      JY=42-IY
      GO TO 50
C
C     2ND QUADRANT
20    IF(IY .EQ. 1) RETURN
      R = RHO(IY,IX)
      THETA = 180.-THT(IY,IX)
      JX = 52-IX
      JY=42-IY
      GO TO 50
C
C     3RD QUADRANT
30    IF(IX .EQ. 1) RETURN
```

```
      R = RHO(IY,IX)
      THETA = 180.+THT(IY,IX)
      JX = 52-IX
      JY=40+IY
      GO TO 50
C
C     4TH QUADRANT
40    IF(IY .EQ. 1) RETURN
      R = RHO(IY,IX)
      THETA = 360.-THT(IY,IX)
      JX = IX+50
      JY=IY+40
50    PRX = FINDP(R,THETA)
      PRISO = PLO
      DO 57 I=1,NPR
      IF(PRX .LE. PRISO) GO TO 58
      PRISO = PRISO+DELP
57    CONTINUE
      I = NPR     +1
58    C(JY,JX) = CPR(I)
      D(JY,JX) = DPR(I)
      RETURN
      END


      FUNCTION FINDP(R,THETA)
      COMMON /PDATA/RAD(10), ANGL(20), PR(10,20), NA,NR
      DIMENSION P(10)
      IPL=0
      ANGLX = THETA
      IF(ANGLX .LT. ANGL(1)) ANGLX = ANGLX+360.
      CALL SRCHX(ANGLX,ANGL,NA,0,ILT,C)
      DO 5 I=1,NR
5     P(I) = PR(I,ILT)+C*(PR(I,ILT+1)-PR(I,ILT))
      FINDP = TLOOK(R,RAD,P,NR,3,0,IPL)
      RETURN
      END


      SUBROUTINE SHADY
      COMMON/PAP/TITLE(48),ICASE
      COMMON/LEGND/CPR(10),DPR(10),PLO,DELP,NPR
      COMMON /PAGE/C(81,101), D(81,101)
      COMMON /PDATA/RAD(10), ANGL(20), PR(10,20), NA,NR
      DIMENSION MB1(40),MB2(43)
      DIMENSION B(2,40)
      INTEGER B
      DATA MB1/15,15,14,14,13,12,11,10,9,6,7*1,
```

```
     A 1,1,1,1,1,1,1,1,1,1,1,1,1,1,1,1,1,1,1,1,1,1,1/
      DATA MB2/50,50,50,50,50,50,49,49,49,49,49,49,49,48,48,47,47,46,46,45,
     A 45,44,43,42,41,40,39,38,37,36,35,33,32,31,29,27,25,22,20,15,10/
      DO 99 N=1,40
      B(1,N)=MB1(N)
   99 B(2,N)=MB2(N)
      DATA BLANK,UP,DOWN/1H ,1H',1H,/
      DATA ISTART/0/
      IDELP=1
      IF(ISTART .EQ. 5) GO TO 25
   31 ISTART=5
      DO 2 I=1,81
      DO 2 J=1,101
      D(I,J) = BLANK
    2 C(I,J) = BLANK
      C(41,51) = UP
      THETA = 0.
      DO 10 I=1,181
      CALL POLRCT(1.,THETA,.25,JX,JY,ICODE)
      IF(ICODE) 7,4,3
    7 C(JY,JX) = DOWN
      GO TO 4
    3 C(JY,JX) = UP
    4 CALL POLRCT(.27,THETA,.25,JX,JY,ICODE)
      IF(ICODE) 8,10,6
    8 C(JY,JX) = DOWN
      GO TO 10
    6 C(JY,JX) = UP
   10 THETA = THETA+2.
   25 SUM = 0.
      NAE = NA-1
      IDELP=1
      PMIN=10.E10
      PMAX=-10.E10
      DO 18 I=1,NR
      DO 18 J=1,NAE
      IF(PR(I,J).LT.PMIN) PMIN=PR(I,J)
      IF(PR(I,J).GT.PMAX) PMAX=PR(I,J)
   18 SUM = SUM+PR(I,J)
      PAVG = SUM/FLOAT(NAE*NR)
      IF(IDELP.GT.0.) GO TO 30
      IDELP=0
      IPLO=PMIN*100.-1.
      PLO=IPLO
      PLO=PLO/100.
      IPMAX=PMAX*100.+1.
      PMAX=IPMAX
      PMAX=PMAX/100.
```

```
      DELP=((PMAX-PLC)*100.)/6.
      IDP=DELP+1.
      DELP=IDP
      DELP=DELP/100.
      IF(DELP.LT..01) DELP=.01
      ZMIN=10.E10
      X=PLC-DELP
      DO 40 I=1,7
      XX=I
      Z=X+XX*DELP-1.
      IF(ABS(Z).LT.ABS(ZMIN)) ZMIN =Z
      IF(Z.EQ.0.) GO TO 41
   40 CONTINUE
      IF(ZMIN.LT.0.) GO TO 42
      PLC=PLC-ZMIN
      GO TO 41
   42 PLC=PLC-ZMIN-DELP
   41 CONTINUE
   30 DO 5 IQ=1,4
      DO 5 IY=1,40
      IXL = B(1,IY)
      IXH = B(2,IY)
      DO 5 IX = IXL,IXH
      CALL CFACE(IX,IY,IQ)
    5 CONTINUE
      CALL CFACE(IX,IY,6)
      WRITE(6,300)(TITLE(I),I=1,48),ICASE
  300 FORMAT(1HC,///,40X,48A1,'CASE',I5)
      WRITE(6,201)(TITLE(I),I=1,48),(C(I,J),J=40,60),ICASE
  201 FORMAT(1H1,48A1,8X,21A1,43X,'CASE ',I4)
      WRITE(6,202) (C(2,J),J=1,101)
  202 FORMAT(1H ,17X,101A1)
      WRITE(6,212) (D(2,J),J=1,101)
  212 FORMAT(1H+,17X,101A1)
      WRITE(6,203) PAVG,(C(3,J),J=1,101)
  203 FORMAT(1H ,7H BASE =,1PE10.3,101A1)
      WRITE(6,212)(D(3,J),J=1,101)
  213 FORMAT(1H+,17X,101A1)
      DO 100 I=4,81
      WRITE(6,202)  (C(I,J),J=1,101)
      WRITE(6,212)(D(I,J),J=1,101)
  100 CONTINUE
      WRITE(6,500)
      WRITE(6,501)
  500 FORMAT(1H ,90X,'ANOTHER PRODUCT OF FUTILITY AIRCRAFT LTD.')
  501 FORMAT(95X,'WEST COAST DIVISION')
      IF(IDELP.EQ.0) DELP=0.
      RETURN
```

```
      END


      SUBROUTINE POLRCT(R,THETA,TCL,JXP,JYP,ICODE)
C     R MUST BE  .LE. 1
      DATA PI/3.14159/
      X = 50.*R*COS(THETA*PI/180.)
      Y = 40.*R*SIN(THETA*PI/180.)
      JX = IFIX(X+.5)
      IF(X .LT. 0.) JX = IFIX(X-.5)
      JY = IFIX(Y+.5)
      IF(Y .LT. 0.) JY = IFIX(Y-.5)
      IF(ABS(X-FLOAT(JX)).GT. TOL .OR. ABS(Y-FLOAT(JY)).GT. TOL)GO TO 5
      JXP = 51+JX
      JYP = 41-JY
      IF(Y .GE. FLOAT(JY)) GO TO 3
      ICODE = -1
      RETURN
3     ICODE = 1
      RETURN
5     ICODE = 0
      RETURN
      END


      FUNCTION TLOOK(P,PT,QT,NT,NP,K,ILAST)
C     PT IS TABLE OF INDEPENDENT VARIABLES
C     QT IS TABLE OF DEPENDENT VARIABLES
C     NT = SIZE OF ABOVE TABLES
C     NP = NUMBER OF POINTS FOR INTERPOLATION
C     K = 0, LIMIT OUTPUT TO BOUNDARY OF TABLE
C     K = 1, EXTRAPOLATE FOR VALUES OUTSIDE TABLE
      DIMENSION PT(1), QT(1), XT(10), YT(10)
      IF(ILAST .LE. 0) ILAST = 1
      I = ILAST+1
      IF(PT(1) - PT(NT)) 4,15,15
C     TABLE PT IS IN ASCENDING ORDER
4     IF(PT(I) .GE. P  .AND.  PT(ILAST) .LE. P) GO TO 8
      DO 5 I=1,NT
      IF(P .LE. PT(I)) GO TO 8
5     CONTINUE
      ILAST = NT-1
6     IF(K .GE. 1) GO TO 7
      TLOOK = QT(NT)
      RETURN
7     IL = NT-NP+1
      GO TO 20
8     IF(I .GT. 1) GO TO 10
```

```
      ILAST = 1
      IF(K .GE. 1) GO TO 9
      TLOCK = QT(1)
      RETURN
9     IL = 1
      GO TO 20
10    ILAST = I-1
      IL = I-NP/2
      GO TO 20
C     TABLE PT IS IN DESCENDING ORDER
15    IF(PT(I) .LE. P  .AND.  PT(ILAST) .GE. P) GO TO 8
      DO 16 I=1,NT
      IF(P .GE. PT(I)) GO TO 8
16    CONTINUE
      GO TO 6
20    IF(IL .LT. 1) IL = 1
      IF(IL .GT. NT-NP+1) IL = NT-NP+1
      DO 21 J = 1,NP
      L = IL+J-1
      XT(J) = PT(L)
21    YT(J) = QT(L)
      CALL LAGRNG(P,Y,XT,YT,NP)
      TLOCK = Y
      RETURN
      END


      SUBROUTINE LAGRNG(X,Y,XT,YT,N)
C
C     THIS ROUTINE USES A LAGRANGIAN POLYNOMIAL BASED ON N TABULAR
C     POINTS TO INTERPOLATE Y AS A FUNCTION OF X IN A TWO DIMENSIONAL
C     TABLE.
C
      DIMENSION XT(1), YT(1)
      DO 1 I=1,N
      IF(X .EQ. XT(I)) GO TO 5
1     CONTINUE
      L1 = 1
      L2 = N-1
      S = (XT(N)-XT(1))/ABS(XT(N)-XT(1))
6     DO 7 I=L1,L2
      IF(ABS(XT(I)-XT(I+1)) .GT. .001*ABS(XT(I))) GO TO 7
      IF((X-XT(I))*S .LE. 0.) GO TO 8
      L1 = I+1
      GO TO 6
8     L2 = I
      GO TO 9
7     CONTINUE
```

```
      L2 = N
9     Y = 0.
      DO 3 I=L1,L2
      Z = 1.
      DO 2 J=L1,L2
      IF(J .EQ. I) GO TO 2
      Z = Z*(X-XT(J))/(XT(I)-XT(J))
2     CONTINUE
3     Y = Y+Z*YT(I)
      RETURN
5     Y = YT(I)
      RETURN
      END


      SUBROUTINE SRCHX(V,VT,N,KEX,IL,C)
C
C     THIS ROUTINE LOCATES V IN TABLE VT
C     IF KEX = 0, LIMIT OUTPUT TO TABLE BOUNDARY
C     IF KEX = 1, EXTRAPOLATE IF V IS OUTSIDE TABLE
      DIMENSION VT(N)
      IF(VT(2) .LT. VT(1)) GO TO 6
C     TABLE VT IS IN ASCENDING ORDER
      DO 1 I=1,N
      IF(V-VT(I)) 2,2,1
1     CONTINUE
15    IL = N-1
      IF(KEX .EQ. 1) GO TO 3
      C = 1.
      RETURN
2     IL = I-1
      IF(I .EQ. 1) GO TO 4
3     C = (V-VT(IL))/(VT(IL+1)-VT(IL))
      RETURN
4     IL = 1
      IF(KEX .EQ. 1) GO TO 3
      C = 0.
      RETURN
C     TABLE VT IS IN DESCENDING ORDER
6     DO 7 I=1,N
      IF(V-VT(I)) 7,2,2
7     CONTINUE
      GO TO 15
      END
//GO.FTO6F001 DD SPACE=(CYL,(1,1)),SYSOUT=O
//GO.FTO4F001 DD UNIT=2400,VOL=SER=NPS223,
//    LABEL=(,SL),DSNAME=INLETD,DISP=(OLD,KEEP),
//    DCB=(RECFM=F,LRECL=1920,BLKSIZE=1920)
```

```
//GO.SYSIN DD *
1418.6713 1418.6713 1451.3273 1496.1226 1636.4836 1694.7291 1694.7291
1405.7029 1405.7029 1455.3907 1582.1753 1728.5401 1707.2761 1707.2761
1332.2134 1332.2134 1466.2439 1543.9504 1596.4982 1698.0627 1698.0627
1327.9400 1327.9400 1499.4361 1527.1232 1712.7689 1689.3808 1689.3808
1380.1003 1380.1003 1415.6249 1512.6465 1642.7130 1662.2269 1662.2269
1408.8715 1408.8715 1480.7541 1601.7068 1690.2755 1716.8910 1716.8910
```

LIST OF REFERENCES

1. AIAA Paper No. 70-632, Distortion and Turbulence Interaction, A Method for Evaluating Engine/Inlet Compatibility, by E. A. Van Deusan and V. R. Mardoc, June 1970.

2. Farmer, C.J., Inlet Distortion, Vorticity, and Stall in an Axial Flow Compressor, Master's Thesis, Naval Postgraduate School, Monterey, Ca., 1972.

3. Brimelow, Brian, Performance Matching of the Propulsion System, SAE preprint 680712, Aeronautics and Space Engineering and Manufacturing Meeting, Los Angeles, Ca., Oct. 7-11, 1968.

4. Private Communication, Paul Burstadt, NASA Lewis Research Center, Cleveland, Ohio, 15 October 1972.

5. AIAA Paper No. 71-667, Instantaneous and Dynamic Analysis of Supersonic Inlet-Engine Compatibility, by J. E. Calogeras, P. L. Burstadt, and R. E. Coltrin, June 1971.

6. Plourde, G. A. and Brimelow, B., Pressure Fluctuations Cause Compressor Instability, paper presented at the Airframe/Propulsion Compatibility Symposium, Wright-Patterson AFB, Ohio, 25 June 1969.

7. AIAA Paper No. 69-488, The Flight Investigation of Pressure Phenomena in the Air Intake of an F-111A Airplane by D. R. Bellman and D. L. Hughes, 1969.

8. AIAA Paper No: 72-1116, A New Approach to Distortion Induced Compressor Stall--Vorticity Maps, by Lt. Clinton Farmer, Lcdr Michael Iverson and Allen Fuhs, 1972.

9. AIAA Paper No. 70-624, Analysis of In-Flight Pressure Fluctuations Leading to Engine Compressor Surge in a F-111A Airplane for Mach Numbers to 2.17, by F. W. Burcham, Jr. and D. L. Hughes, June 1970.

10. AIAA Paper No. 72-37, A Method for Analyzing Dynamic Stall by Peter Crimi and Barry L. Reeves, January 1972.

11. AIAA Paper No. 71-669, Experimental Evaluation of a Hypothesis for Scaling Inlet Turbulence Data, by D. A. Sherman, D. L. Motycka and G. C. Oates, June 1971.

12. AIAA Paper No. 71-670, Compressor Sensitivity to Transient and Distorted Transient Flows, by W. Jansen, M. C. Swarden, and A. W. Carlson, June 1971.

13. Brownstein, B. J., A Universal Inlet Distortion Factor System, 1972.

14. Farmer, C. J., Iverson, M. M., and Fuhs, A. E., Inlet Distortion Vorticity and Compressor Stall, Naval Postgraduate School, Monterey, Ca., 1972.

15. Carta, F. O., "Unsteady Force on an Airfoil in a Periodically Stalled Inlet Flow," Journal of Aircraft v. 4, p. 416-421, October 1967.

16. Ericsson, L. E. and Reding, J. P., "Unsteady Airfoil Stall, Review and Extension," Journal of Aircraft, v. 8, p. 609-616, 1971.

17. Carta, F. O., "Effect of Unsteady Pressure Gradient Reduction on Dynamic Stall Delay," Journal of Aircraft, v. 8, p. 839-841, 1971.

18. Houghton, E. L. and Brock, A. E., Aerodynamics for Engineering Students, Edward Arnold, 1960.

INITIAL DISTRIBUTION LIST

		No. Copies
1.	Defense Documentation Center Cameron Station Alexandria, Virginia 22314	2
2.	Library, Code 0212 Naval Postgraduate School Monterey, California 93940	2
3.	Chairman, Department of Aeronautics Naval Postgraduate School Monterey, California 93940	1
4.	Professor Allen E. Fuhs Department of Aeronautics Naval Postgraduate School Monterey, California 93940	10
5.	Ens. James E. Shoemaker 113 Norton Street Bennington, Vermont 05201	3
6.	Professor M. H. Vavra Department of Aeronautics Naval Postgraduate School Monterey, California 93940	1
7.	Professor M. F. Platzer Department of Aeronautics Naval Postgraduate School Monterey, California 93940	1
8.	RADM Carl O. Holmquist, USN Chief of Naval Research Office of Naval Research Arlington, Virginia 22218	1
9.	Captain William Sallada, USN Office of Naval Research Arlington, Virginia 22218	1
10.	Mr. Joe Boytos Naval Air Propulsion Test Center Trenton, New Jersey 08628	1

11. Dr. Herbert Mueller — 1
Code 310A
Naval Air Systems Command
Washington, D. C. 20360

12. Mr. Irv Silver — 1
Code 03B
Naval Air Systems Command
Washington, D. C. 20360

13. Dr. Frank Tanczos — 1
Code 03
Naval Air Systems Command
Washington, D. C. 20360

14. Mr. Karl Guttman — 1
Code 330
Naval Air Systems Command
Washington, D. C. 20360

15. Dr. H. O. Johnson — 1
Code 330
Naval Air Systems Command
Washington, D. C. 20360

16. Mr. Robert Brown — 1
Code 536
Naval Air Systems Command
Washington, D. C. 20360

17. Dr. John A. Satkowski — 1
Power Program
Office of Naval Research
Arlington, Virginia 22217

18. Dr. Ralph Roberts — 1
Office of Naval Research
800 North Quincy Street
Arlington, Virginia 22217

19. Mr. Eric Lister — 1
R. & T. Division
Naval Air Propulsion Test Center
Trenton, New Jersey 08628

20. Mr. Albert Martino — 1
R. & T. Division
Naval Air Propulsion Test Center
Trenton, New Jersey 08628

21. Mr. James Patton, Jr. — 1
Office of Naval Research
Arlington, Virginia 22218

22. Dr. Peter Crimi — 1
AVCO Systems Div.
201 Lowell Street
Wilmington, Mass. 01887

23. M. l'Ingenieur en Chef Marc Pianko — 1
Service Technique Aeronautique
4 Avenue de la Porte d'Issy
75 Paris 15eme FRANCE

24. Mr. J. Surugue — 1
Directeur, Energie et Propulsion
ONERA
29 Avenue de la Division Leclerc
92 Chatillon-sous-Bagneux, FRANCE

25. Dr. Dunham — 1
National Gas Turbine Establishment
Pyestock
Farnborough Hants GREAT BRITAIN

26. Professor Kuhl — 1
D. V. L.
505 Porz Wahn
Linder Hohe
Allemagne GERMANY

27. Mr. Clifford Simpson — 1
AFAPL/TB
Wright-Patterson A.F.B., Ohio 45433

28. Professor Gordon Oates — 1
University of Washington
Seattle, Washington 98105

29. Professor Robert Goulard — 1
Director, Project SQUID
Purdue University
Lafayette, Indiana

30. Mr. J. F. Chevalier — 1
SNECMA
Centre d'Essais de Villaroche
77 Moissy-Cramayel FRANCE

31. Mr. M. Van Staveren — 1
Institute for Applied Research TNO
Post bus 406
Delft NETHERLANDS

32. Mr. Hill Barrett — 1
Detroit Diesel Allison
General Motors Corp.
Indianapolis, Indiana 46206

33. Professor Antonia Ferri — 1
Department of Aeronautics and Astronautics
School of Engineering and Science
New York University
Bronx, New York 10453

34. Mr. Elmer G. Johnson — 1
Director, Fluid Dynamics Facilities Research Laboratory
USAF Aerospace Research Laboratories
WPAFB, Ohio 45433

35. Mr. Marvin Stibich — 1
Turbine Engine Division
AFAPL
WPAFB, Ohio 45433

36. Dr. A. A. Mikolajczak — 1
Pratt and Whitney Aircraft
East Hartford, Conn. 06108

37. Dr. Peter Trimm — 1
Detroit Diesel Allison
General Motors Corp.
Indianapolis, Indiana 46206

38. Professor Duncan Rannie — 1
California Institute of Technology
Pasadena, California 91109

39. Professor Jack Kerrebrock — 1
Aeronautics and Astronautics
Massachusetts Institute of Technology
Cambridge, Massachusetts 02138

40. Professor George Serovy — 1
Iowa State University
Ames, Iowa 50010

41. Professor Alan Stenning — 1
Lehigh University
Bethlehem, Pennsylvania 18015

42. Dr. Gary R. Ludwig — 1
Aerodynamics Research
Cornell Aeronautical Laboratory, Inc.
Buffalo, New York 14221

43. Mr. James E. Calogeras — 1
NASA Lewis Research Center
Cleveland, Ohio 44135

44. Mr. F. E. Schubert — 1
AFAPL/TB
Wright-Patterson AFB, Ohio 45433

45. Dr. Gunnar Broman — 1
Vice President, Engineering
VOLVO Flygmotor
Trollhattan, SWEDEN

46. Mr. Robert Zalis — 1
MZ 240 GF
1000 Western Avenue
Lynn, Massachusetts 01910

47. Mr. Paul H. Kutschenreuter, Jr. — 1
Mail Drop E 198
General Electric Company
Cincinnati, Ohio 45215

48. Mr. David Jamison — 1
General Electric Company
P. O. Box 2143
Kettering Branch
Dayton, Ohio 45429

49. Prof. Jacques Valensi — 1
Director Institut de Mecanique des Fluides
l'Universite d'Aix-Marseille
Marseille, FRANCE

50. Professor Jacques Chauvin — 1
Von Karman Institute for Fluid Mechanics
72 Chaussee de Waterloo
1640 Rhode-St-Genese BELGIUM

51. Mr. Marvin F. Schmidt — 1
Turbine Engine Division
AFAPL
WPAFB, Ohio 45433

52. Mr. J. W. McBride — 1
General Electric Company
Evandale, Ohio 45215

53. Dr. Leroy H. Smith, Jr. — 1
General Electric Company
Evandale, Ohio 45215

54. Professor B. Lakshminarayana 1
MIT Gas Turbine Laboratory
Massachusetts Institute of Technology
Cambridge, Massachusetts 02138

55. Professor Jean Louis 1
MIT Gas Turbine Laboratory
Massachusetts Institute of Technology
Cambridge, Massachusetts 02138

56. Dr. F. O. Carta 1
United Aircraft Research Labs.
United Aircraft Corporation
400 Main Street
East Hartford, Connecticut 06108

57. Mr. Norman Cotter 1
Pratt and Whitney Florida Research Center
West Palm Beach, Florida 33402

58. Dr. George L. Mellor 1
Princeton University
Forrestal Campus
Princeton, New Jersey 08540

59. Mr. Stan Ellis 1
Pratt and Whitney Florida Research Center
West Palm Beach, Florida 33402

60. Mr. David Bowditch 1
NASA Lewis Research Center
Cleveland, Ohio 44135

61. Professor Frank Marble 1
California Institute of Technology
Pasadena, California 91109

62. Dr. W. Z. Sadeh 1
Engineering Research Center
Colorado State University
Ft. Collins, Colorado 80521

63. Professor Bruce A. Reese 1
School of Mechanical Engineering
Purdue University
Lafayette, Indiana 47907

64. Professor P. C. Adamson, Jr. 1
Dept. of Aerospace Engineering
University of Michigan
Ann Arbor, Michigan 48103

65. Professor W. R. Sears — 1
Grumman Hall
Cornell University
Ithaca, New York 14850

66. Professor J. E. McCune — 1
M.I.T. - 37 - 391
Cambridge, Massachusetts 02139

67. Dr. Jack Nielsen — 1
Nielsen Engineering and Research, Inc.
850 Maude Avenue
Mountain View, California 94040

68. John Scott — 1
School of Engineering and Applied Science
University of Virginia
Charlottesville, Virginia 22901

69. W. F. O'Brien — 1
Mechanical Engineering Dept.
Virginia Polytechnic Institute and State University
Blacksburg, Virginia 24061

70. Dr. W. Heiser — 1
AFAPL
WPAFB, Ohio 45433

71. J. P. Johnston — 1
Mechanical Engineering Dept.
Stanford University
Stanford, California

72. CAPT Barry Brownstein — 1
Air Force Aero-Propulsion Laboratory
Wright-Patterson A.F.B, Ohio 45433

UNCLASSIFIED

Security Classification

DOCUMENT CONTROL DATA - R & D

(Security classification of title, body of abstract and indexing annotation must be entered when the overall report is classified)

ORIGINATING ACTIVITY (Corporate author)

Naval Postgraduate School
Monterey, California 93940

2a. REPORT SECURITY CLASSIFICATION
Unclassified

2b. GROUP

REPORT TITLE

An Analytical Analysis of the Effects of Instantaneous Vorticity on Compressor Performance

DESCRIPTIVE NOTES (Type of report and inclusive dates)

Master's Thesis, June 1973

AUTHOR(S) (First name, middle initial, last name)

James E. Shoemaker

REPORT DATE	7a. TOTAL NO. OF PAGES	7b. NO. OF REFS
June 1973	94	18

CONTRACT OR GRANT NO.

PROJECT NO.

9a. ORIGINATOR'S REPORT NUMBER(S)

9b. OTHER REPORT NO(S) (Any other numbers that may be assigned this report)

DISTRIBUTION STATEMENT

Approved for public release; distribution unlimited.

SUPPLEMENTARY NOTES

12. SPONSORING MILITARY ACTIVITY
Naval Postgraduate School
Monterey, California 93940

ABSTRACT

Vorticity forms the basis for a new approach to the analysis of inlet distortion in axial flow fans and compressors. Farmer first formulated this approach and this paper represents a test of the usefulness of his theory. A summary of recent developments in the field along with a discussion of the effects of distortion on stall margin forms a background for this complex problem. A computer program calculates the vorticity pattern at the compressor face using data that are read from a magnetic tape. The data, which were provided by NASA Lewis Research Center in Cleveland, consist of eleven stall events. The output of the program contains tables of stagnation pressure and the partial derivatives of pressure in the R and theta directions as well as three maps. The three maps are of pressure and radial and circumferential vorticity. The results of the program show a correlation between a ring of large positive circumferential vorticity and stall, leading to the conclusion that the stall was caused by the increase in blade loading induced by the vorticity. This conclusion suggests a formulation for a universal inlet distortion index and provices a basis for the evaluation of the vorticity approach to the problem.

DD FORM 1 NOV 68 1473 (PAGE 1)

S/N 0101-807-6811

UNCLASSIFIED

Security Classification

A-31408

KEY WORDS	LINK A		LINK B		LINK C	
	ROLE	WT	ROLE	WT	ROLE	WT
STALL						
VORTICITY PATTERN						
DISTORTION INDEX						

Thesis
S4782 Shoemaker
c.1
145378
An analytical analysis of the effects of instantaneous vorticity on compressor performance.